Please cite this article in press as: Warren et al., Highly Efficient Reprogramming to Pluripotency and Directed Differentiation of Human Cells with Synthetic Modified mRNA, Cell Stem Cell (2010), doi:10.1016/j.stem.2010.08.012

Cell Stem Cell
Article

Highly Efficient Reprogramming to Pluripotency and Directed Differentiation of Human Cells with Synthetic Modified mRNA

Luigi Warren,[1,17] Philip D. Manos,[2,4,17] Tim Ahfeldt,[4,6,7] Yuin-Han Loh,[8,9] Hu Li,[11,12] Frank Lau,[4,13] Wataru Ebina,[1] Pankaj K. Mandal,[1] Zachary D. Smith,[14] Alexander Meissner,[4,5,14] George Q. Daley,[2,3,4,5,8,15,16] Andrew S. Brack,[5,6] James J. Collins,[11,12,15] Chad Cowan,[4,5,6,13] Thorsten M. Schlaeger,[2,8] and Derrick J. Rossi[1,2,5,10,*]

[1]Immune Disease Institute, Program in Cellular and Molecular Medicine
[2]Stem Cell Program
[3]Manton Center for Orphan Disease Research
Children's Hospital Boston, Boston, MA 02115, USA
[4]Department of Stem Cell and Regenerative Biology
[5]Harvard Stem Cell Institute
Harvard University, Cambridge, MA 02138, USA
[6]Center of Regenerative Medicine, Massachusetts General Hospital, 185 Cambridge Street, Boston, MA 02114-2790, USA
[7]Department of Biochemistry and Molecular Biology II: Molecular Cell Biology, University Medical Center Hamburg-Eppendorf, Hamburg 20246, Germany
[8]Division of Pediatric Hematology/Oncology, Children's Hospital Boston and Dana-Farber Cancer Institute, Boston, MA 02115, USA
[9]Department of Biological Chemistry and Molecular Pharmacology
[10]Department of Pathology
Harvard Medical School, Boston, MA 02115, USA
[11]Department of Biomedical Engineering and Center for BioDynamics, Boston University, Boston, MA 02215, USA
[12]Wyss Institute for Biologically Inspired Engineering, Harvard University, Boston, MA 02115, USA
[13]Stowers Medical Institute, 185 Cambridge Street, Boston, MA 02114, USA
[14]Broad Institute of MIT and Harvard, Cambridge, MA 02142, USA
[15]Howard Hughes Medical Institute
[16]Division of Hematology/Oncology, Brigham and Women's Hospital, Boston, MA 02115, USA
[17]These authors contributed equally to this work
*Correspondence: rossi@idi.harvard.edu
DOI 10.1016/j.stem.2010.08.012

SUMMARY

Clinical application of induced pluripotent stem cells (iPSCs) is limited by the low efficiency of iPSC derivation and the fact that most protocols modify the genome to effect cellular reprogramming. Moreover, safe and effective means of directing the fate of patient-specific iPSCs toward clinically useful cell types are lacking. Here we describe a simple, nonintegrating strategy for reprogramming cell fate based on administration of synthetic mRNA modified to overcome innate antiviral responses. We show that this approach can reprogram multiple human cell types to pluripotency with efficiencies that greatly surpass established protocols. We further show that the same technology can be used to efficiently direct the differentiation of RNA-induced pluripotent stem cells (RiPSCs) into terminally differentiated myogenic cells. This technology represents a safe, efficient strategy for somatic cell reprogramming and directing cell fate that has broad applicability for basic research, disease modeling, and regenerative medicine.

INTRODUCTION

The reprogramming of differentiated cells to pluripotency holds great promise as a tool for studying normal development, while offering hope that patient-specific induced pluripotent stem cells (iPSCs) could be used to model disease or to generate clinically useful cell types for autologous therapies aimed at repairing deficits arising from injury, illness, and aging. Induction of pluripotency was originally achieved by Yamanaka and colleagues by enforced expression of four transcription factors, KLF4, c-MYC, OCT4, and SOX2 (KMOS), by using retroviral vectors (Takahashi et al., 2007; Takahashi and Yamanaka, 2006). Viral integration into the genome initially presented a formidable obstacle to therapeutic use of iPSCs. The search for ways to induce pluripotency without incurring genetic change has thus become the focus of intense research effort. Toward this end, iPSCs have been derived via excisable lentiviral and transposon vectors or through repeated application of transient plasmid, episomal, and adenovirus vectors (Chang et al., 2009; Kaji et al., 2009; Okita et al., 2008; Stadtfeld et al., 2008; Woltjen et al., 2009; Yu et al., 2009). iPSCs have also been derived with two DNA-free methods: serial protein transduction with recombinant proteins incorporating cell-penetrating peptide moieties (Kim et al., 2009; Zhou et al., 2009) and transgene

Please cite this article in press as: Warren et al., Highly Efficient Reprogramming to Pluripotency and Directed Differentiation of Human Cells with Synthetic Modified mRNA, Cell Stem Cell (2010), doi:10.1016/j.stem.2010.08.012

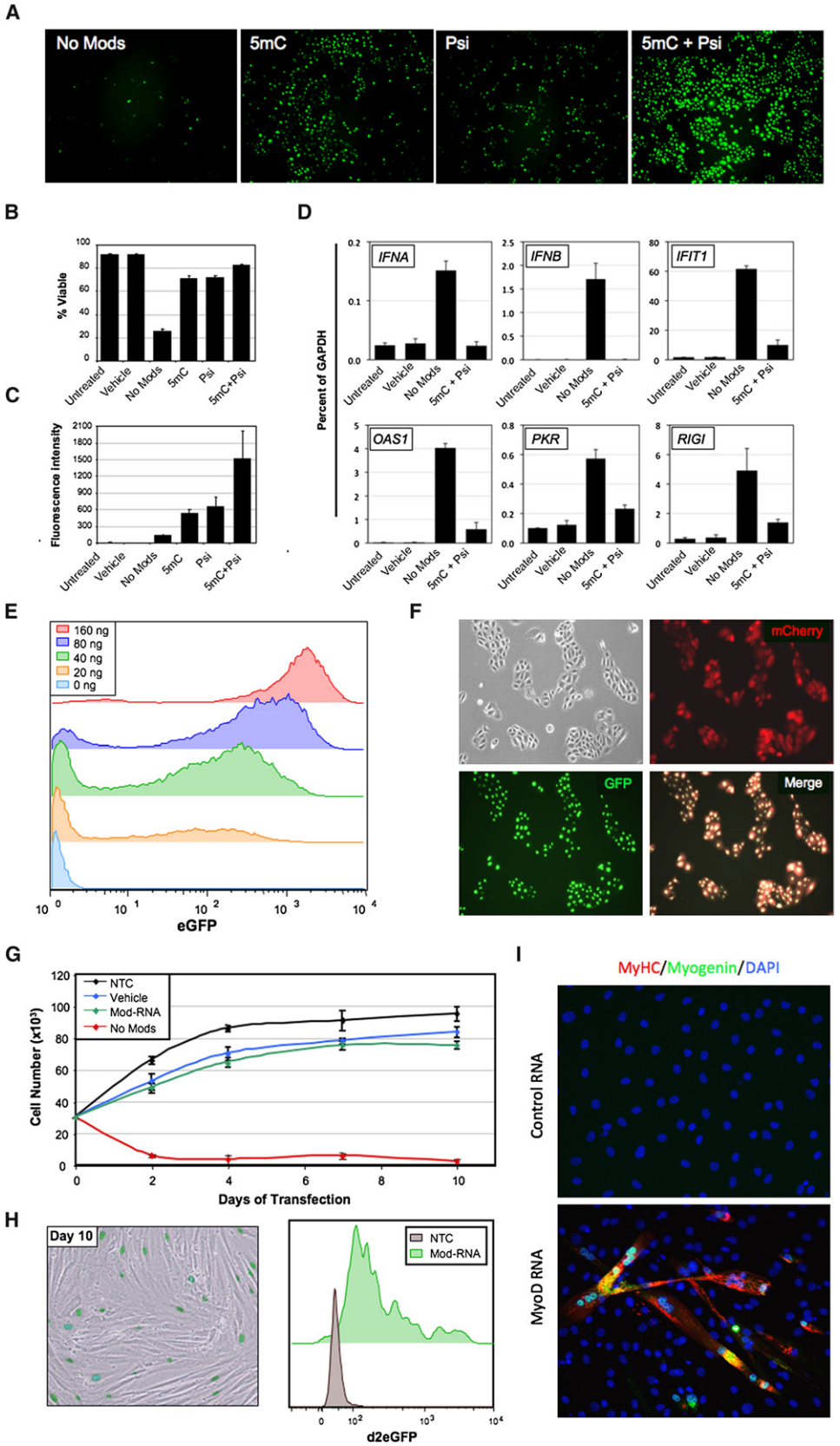

delivery using the Sendai virus, which has a completely RNA-based reproductive cycle (Fusaki et al., 2009).

Despite such progress, considerable limitations accompany the nonintegrative iPSC derivation strategies devised thus far. For example, although DNA transfection-based methodologies are ostensibly safe, they nonetheless entail some risk of genomic recombination or insertional mutagenesis. In protein-based strategies, the recombinant proteins used are challenging to generate and purify in the quantities required (Zhou et al., 2009). Use of Sendai virus requires stringent steps to purge reprogrammed cells of replicating virus, and the sensitivity of the viral RNA replicase to transgene sequence content may limit the generality of this reprogramming vehicle (Fusaki et al., 2009). Importantly, methods that rely on repeat administration of transient vectors, whether DNA or protein based, have so far shown very low iPSC derivation efficiencies (Jia et al., 2010; Kim et al., 2009; Okita et al., 2008; Stadtfeld et al., 2008; Yu et al., 2009; Zhou et al., 2009), presumably because of weak or inconstant expression of reprogramming factors.

Here we demonstrate that repeated administration of synthetic messenger RNAs incorporating modifications designed to bypass innate antiviral responses can reprogram differentiated human cells to pluripotency with conversion efficiencies and kinetics substantially superior to established viral protocols. Furthermore, this simple, nonmutagenic, and highly controllable technology is applicable to a range of tissue-engineering tasks, exemplified here by RNA-mediated directed differentiation of RNA-iPSCs (RiPSCs) to terminally differentiated myogenic cells.

RESULTS

Development of Modified RNAs for Directing Cell Fate

We manufactured mRNA by using in vitro transcription (IVT) reactions templated by PCR amplicons (Figure S1 available online). To promote efficient translation and boost RNA half-life in the cytoplasm, a 5′ guanine cap was incorporated by inclusion of a synthetic cap analog in the IVT reactions (Yisraeli and Melton, 1989). Within our IVT templates, the open reading frame (ORF) of the gene of interest is flanked by a 5′ untranslated region (UTR) containing a strong Kozak translational initiation signal and an alpha-globin 3′ UTR terminating with an oligo(dT) sequence for templated addition of a polyA tail.

Cytosolic delivery of mRNA into mammalian cells can be achieved via electroporation or by complexing the RNA with a cationic vehicle to facilitate uptake by endocytosis (Audouy and Hoekstra, 2001; Elango et al., 2005; Holtkamp et al., 2006; Van den Bosch et al., 2006; Van Tendeloo et al., 2001). We focused on the latter approach, reasoning that this would allow for repeated transfection to sustain ectopic protein expression over the days to weeks required for cellular reprogramming. In preliminary experiments in which synthetic RNA encoding GFP was transfected into murine embryonic fibroblasts and human epidermal keratinocytes, a high, dose-dependent cytotoxicity was observed that was not attributable to the cationic vehicle, which was exacerbated on repeated transfection. These experiments revealed a serious impediment to achieving sustained protein expression by mRNA transfection and highlighted a need to develop a technology that would permit sustained protein expression with mRNA with reduced cellular toxicity.

It is known that exogenous single-stranded RNA (ssRNA) activates antiviral defenses in mammalian cells through interferon- and NF-κB-dependent pathways (Diebold et al., 2004; Hornung et al., 2006; Kawai and Akira, 2007; Pichlmair et al., 2006; Uematsu and Akira, 2007). We sought approaches to reduce the immunogenic profile of synthetic RNA in order to increase the sustainability of RNA-mediated protein expression. Cotranscriptional capping yields a significant fraction of uncapped IVT products bearing 5′ triphosphates, which can be detected by the ssRNA sensor RIG-I (Hornung et al., 2006; Pichlmair et al., 2006), and have also been reported to activate PKR, a global repressor of protein translation (Nallagatla and Bevilacqua, 2008). We therefore treated synthesized RNA with a phosphatase, which resulted in modest reductions in cytotoxicity upon transfection (data not shown).

Eukaryotic mRNA is extensively modified in vivo, and the presence of modified nucleobases has been shown to reduce signaling by RIG-I and PKR, as well as by the less widely expressed but inducible endosomal ssRNA sensors TLR7 and TLR8 (Karikó et al., 2005, 2008; Karikó and Weissman, 2007; Nallagatla and Bevilacqua, 2008; Nallagatla et al., 2008; Uzri and Gehrke, 2009). In an attempt to further reduce innate immune responses to transfected RNA, we synthesized mRNAs incorporating modified ribonucleoside bases. Complete substitution of either 5-methylcytidine (5mC) for cytidine or pseudouridine (psi) for uridine in GFP-encoding transcripts markedly improved viability and increased ectopic protein expression, although the most significant improvement was seen when both modifications were used together (Figures 1A–1C). These modifications dramatically attenuated interferon signaling as revealed by qRT-PCR for a panel of interferon response genes,

Figure 1. Modified RNA Overcomes Antiviral Responses and Can Be Used to Direct Cell Fate

(A) Microscopy images showing keratinocytes transfected 24 hr earlier with 400 ng/well of synthetic unmodified (No Mods), 5-methyl-cytosine modified (5mC), pseudouridine modified (Psi), or 5mC + Psi modified RNA encoding GFP.

(B and C) Percent viability (B) and mean fluorescence intensity (C) of the cells shown in (A) as measured by flow cytometry.

(D) Quantitative RT-PCR data showing expression of six interferon-regulated genes in BJ fibroblasts 24 hr after transfection with unmodified (No Mods) or modified (5mC + Psi) RNA encoding GFP (1200 ng/well), and vehicle and untransfected controls.

(E) Flow cytometry histograms showing GFP expression in keratinocytes transfected with 0–160 ng of modified-RNA, 24 hr posttransfection.

(F) Microscopy images of keratinocytes cotransfected with modified RNAs encoding GFP with a nuclear localization signal, and mCherry (cytosolic) proteins.

(G) Growth kinetics of BJ fibroblasts transfected daily with unmodified or modified RNAs encoding a destabilized nuclear-localized GFP, and vehicle and untransfected controls for 10 days.

(H) Sustained GFP expression of modified RNA-transfected cells described in (G) at day 10 of transfection shown by fluorescence imaging with bright field overlay (left) and flow cytometry (right).

(I) Immunostaining for the muscle-specific proteins myogenin and myosin heavy chain (MyHC) in murine C3H/10T1/2 cell cultures 3 days after three consecutive daily transfections with a modified RNA encoding *MYOD*.

Error bars indicate SD, n = 3 for all panels. See also Figure S2.

Please cite this article in press as: Warren et al., Highly Efficient Reprogramming to Pluripotency and Directed Differentiation of Human Cells with Synthetic Modified mRNA, Cell Stem Cell (2010), doi:10.1016/j.stem.2010.08.012

although residual upregulation of some interferon targets was still detected (Figure 1D). It is known that cellular antiviral defenses can self-prime through a positive-feedback loop involving autocrine and paracrine signaling by type I interferons (Randall and Goodbourn, 2008). Media supplementation with a recombinant version of B18R protein, a Vaccinia virus decoy receptor for type I interferons (Symons et al., 1995), further increased cell viability of RNA transfection in some cell types (data not shown). Synthesis of RNA with modified ribonucleotides and phosphatase treatment (henceforth, modified RNAs), used in conjunction with media supplementation with the interferon inhibitor B18R, allowed for high, dose-dependent levels of protein expression with high cell viability (Figure 1E).

Transfection of modified RNA encoding GFP into six human cell types showed highly penetrant expression (50%–90% positive cells), demonstrating the applicability of this technology to diverse cell types (Figure S2A). Simultaneous delivery of modified RNAs encoding mCherry and GFP containing a nuclear localization signal confirmed that generalized coexpression of multiple proteins could be achieved in mammalian cells and that expressed proteins could be correctly localized to different cellular compartments (Figure 1F). Ectopic protein expression after RNA transfection is transient owing to RNA and protein degradation and the diluting effect of cell division. To establish the kinetics and persistence of protein expression, modified RNA encoding GFP variants designed for high and low protein stability (Li et al., 1998) were synthesized and transfected into keratinocytes. Time course analysis by flow cytometry showed that protein expression persisted for several days for the high-stability variant but peaked within 12 hr and decayed rapidly thereafter for the destabilized GFP (Figure S2B). These results indicated that a repetitive transfection regimen would be required to sustain high levels of ectopic expression for short-lived proteins over an extended time course. To address this and further examine the impact of repeated RNA transfection on cell growth and viability, we transfected BJ fibroblasts for 10 consecutive days with either unmodified or modified RNAs encoding a destabilized nuclear GFP and appropriate controls (Figure S3A). Daily transfection with modified RNA permitted sustained protein expression without substantially compromising the viability of the culture beyond a modest reduction in growth kinetics that was largely attributable to the transfection reagent (Figures 1G and 1H; Figure S2C). Microarray analysis of the cultures after the tenth and final transfection revealed that prolonged daily transfection with modified RNA did not significantly alter the molecular profile of the transfected cells (Figure S2D), although upregulation of a number of interferon response genes was noted, consistent with our previous observation that the RNA modifications did not completely abrogate interferon signaling (Figure 1D; Figure S2E). By contrast, repeated transfection with unmodified RNA severely compromised the growth and viability of the culture through elicitation of a massive interferon response (Figure 1D), indicating that the use of unmodified RNA was not a viable strategy for sustaining polypeptide expression in cells (Figure 1G).

To determine whether modified RNAs could be used to directly alter cell fate, we synthesized modified RNA encoding the myogenic transcription factor *MYOD* (Davis et al., 1987) and transfected it into murine C3H10T1/2 cells over the course of 3 days, followed by continued culturing in a low serum media for an additional 3 days. The emergence of large, multinucleated myotubes that stained positive for the myogenic markers myogenin and myosin heavy chain (MyHC) provided proof of principle that transfection with modified RNAs could be utilized to efficiently direct cell fate (Figure 1I).

Generation of Induced Pluripotent Stem Cells via Modified RNAs

We next sought to determine whether induced pluripotent stem cells (iPSCs) could be derived via modified RNAs. To this end, modified RNAs encoding the four canonical Yamanaka factors, *KLF4* (K), *c-MYC* (M), *OCT4* (O), and *SOX2* (S), were synthesized and transfected into cells. Immunostaining with antibodies directed against OCT4, KLF4, and SOX2 demonstrated that each of the factors was robustly expressed and correctly localized to the nucleus (Figure 2A). Expression kinetics was monitored by flow cytometry, which showed maximal protein expression 12 to 18 hours after transfection, followed by rapid turnover of these transcription factors (Figure 2B). From this we concluded that daily transfections would be required to maintain high levels of expression of the Yamanaka factors during long-term, multifactor reprogramming regimens.

We next sought to establish a protocol to ensure sustained, high-level protein expression through daily transfection of modified RNAs by exploring a matrix of conditions encompassing different transfection reagents, culture media, feeder cell types, and RNA doses (data not shown). Once optimized, we initiated long-term reprogramming experiments with human ESC-derived dH1f fibroblasts, which display relatively efficient viral-mediated iPSC conversion (Chan et al., 2009; Park et al., 2008). Low-oxygen (5% O_2) culture conditions and a KMOS stoichiometry of 1:1:3:1 were employed, because these have been reported to promote efficient iPSC conversion (Kawamura et al., 2009; Papapetrou et al., 2009; Utikal et al., 2009; Yoshida et al., 2009). Modified RNA encoding a destabilized nuclear GFP was spiked into the KMOS RNA cocktail to allow visualization of continued protein expression throughout the experimental time course (Figure S3A). Widespread transformation of fibroblast morphology to a compact, epithelioid morphology was observed within the first week of modified RNA transfection, followed by emergence of canonical hESC-like colonies with tight morphology, well-defined borders, and prominent nucleoli toward the end of the second week of transfection (Figure 2C). RNA transfection was terminated on day 17, and colonies were mechanically picked 3 days later, which were then expanded under standard ESC culture conditions to establish 14 prospective iPSC lines, designated dH1f-RiPSC (RNA-derived iPSC) 1–14.

We next attempted to reprogram somatically derived cells to pluripotency by using a similar reprogramming regimen. Anticipating that these cells might be more challenging to reprogram, we employed a five-factor cocktail including a modified RNA encoding LIN28 (KMOSL), which has been shown to facilitate reprogramming (Yu et al., 2007; Hanna et al., 2009), and we supplemented the media with valproic acid (VPA), a histone deacetylase inhibitor that has been reported to increase reprogramming efficiency (Huangfu et al., 2008). Four human cell types were tested: Detroit 551 (D551) and MRC-5 fetal fibroblasts, BJ

Please cite this article in press as: Warren et al., Highly Efficient Reprogramming to Pluripotency and Directed Differentiation of Human Cells with Synthetic Modified mRNA, Cell Stem Cell (2010), doi:10.1016/j.stem.2010.08.012

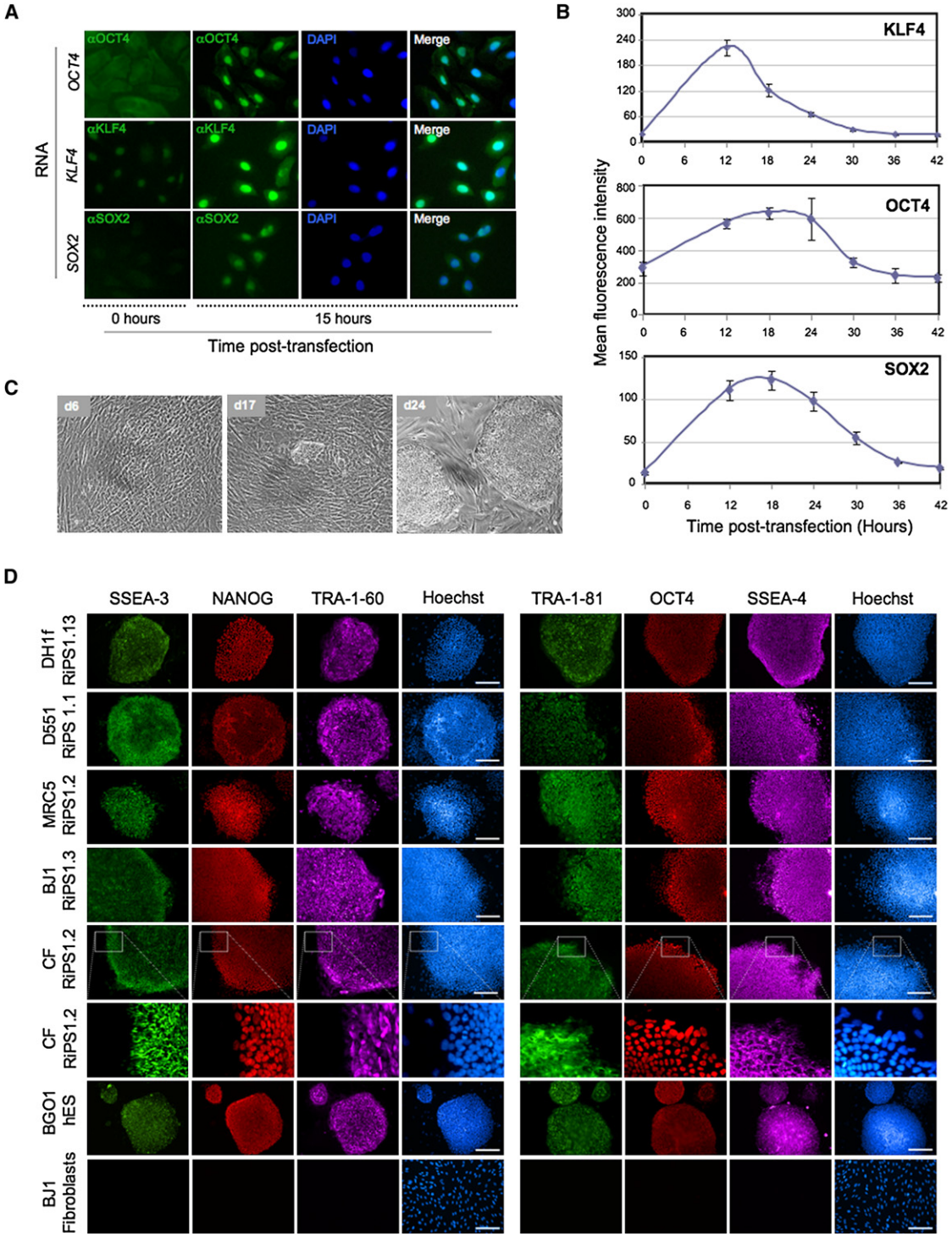

Figure 2. Generation of RNA-Induced Pluripotent Stem Cells

(A) Immunostaining for human KLF4, OCT4, and SOX2 proteins in keratinocytes 15 hr posttransfection with modified RNA encoding KLF4, OCT4, or SOX2.

(B) Time course showing kinetics and stability of KLF4, OCT4, and SOX2 proteins after modified RNA transfection, assayed by flow cytometry after intracellular staining of each protein.

(C) Bright-field images taken during the derivation of RNA-iPSCs (RiPS) from dH1f fibroblasts showing early epitheliod morphology (day 6), small hESC-like colonies (day 17), and appearance of mature iPSC clones after mechanical picking and expansion (day 24).

(D) Immunohistochemistry showing expression of a panel of pluripotency markers in expanded RiPSC clones derived from dH1f fibroblasts, Detroit 551 (D551) and MRC-5 fetal fibroblasts, BJ postnatal fibroblasts, and cells derived from a skin biopsy taken from an adult cystic fibrosis patient (CF), shown also in high magnification. BG01 hESCs and BJ1 fibroblasts are included as positive and negative controls, respectively. Scale bars represent 200 μm.

See also Figures S3 and S4.

Please cite this article in press as: Warren et al., Highly Efficient Reprogramming to Pluripotency and Directed Differentiation of Human Cells with Synthetic Modified mRNA, Cell Stem Cell (2010), doi:10.1016/j.stem.2010.08.012

postnatal fibroblasts, and fibroblast-like cells cultured from a primary skin biopsy taken from an adult cystic fibrosis patient (CF cells). Daily transfection with the modified RNA KMOSL cocktail gave rise to numerous hESC-like colonies in the D551, BJ, CF, and MRC5 cultures that were mechanically picked at day 18, 20, 21, and 25, respectively. More than 10 RiPSC clones were expanded for each of the somatic lines, with notably very few clones failing to establish. Immunostaining confirmed the expression of OCT4, NANOG, TRA-1-60, TRA-1-81, SSEA3, and SSEA4 in all the RiPSC lines examined (Figure 2D; Figure S3B). DNA fingerprinting confirmed parental origin of three RiPSC clones from each somatic cell derivation, and all clones presented normal karyotypes (data not shown). Of note, additional experiments conducted in the presence or absence of VPA showed little difference in reprogramming efficiency (data not shown), and VPA was therefore not used in subsequent experiments.

Molecular Characterization and Functional Potential of RiPSCs

A number of molecular and functional assays were performed to further assess whether the RiPSCs had been reprogrammed to pluripotency (Table S1). Multiple RiPSC lines derived from each of the five starting cell types were evaluated by quantitative RT-PCR (qRT-PCR), and all demonstrated robust expression of the pluripotency-associated transcripts *OCT4*, *SOX2*, *NANOG,* and *hTERT* (Figure 3A). Bisulfite sequencing of the Oct4 locus revealed extensive demethylation relative to the parental fibroblasts, an epigenetic state equivalent to human ESCs (Figure 3B).

To gain more global insight into the molecular properties of RiPSCs, gene expression profiles of RiPSC clones from multiple independent derivations were generated and compared to fibroblasts, human ESCs, and virally derived iPSC lines. These analyses revealed that all modified RNA-derived iPSC clones examined had a molecular signature that very closely recapitulated that of human ESCs while being highly divergent from the profile of the parental fibroblasts (Figure 3C). Importantly, pluripotency-associated transcripts including *SOX2, REX1, NANOG, OCT4, LIN28*, and *DNMT3B* were substantially upregulated in the RiPSCs compared to the parental fibroblast lines to levels comparable to hESCs (Figure 3C). Furthermore, when the transcriptional profiles were subjected to unsupervised hierarchical clustering analysis, all RiPSC clones analyzed clustered more closely to hESC than did virally derived iPSCs, suggesting that modified RNA-derived iPSCs more fully recapitulated the molecular signature of human ESCs (Figure 3D).

To test the developmental potential of RiPSCs, embryoid bodies (EBs) were generated from multiple clones from five independent RiPSC derivations, and beating cardiomyocytes were observed for the vast majority of the EBs (Table S1, Movie S1). Mesodermal potential was further evaluated in methylcellulose blood-forming assays that showed that all lines tested were robustly able to differentiate into hematopoietic precursors capable of giving rise to colony numbers and a spectrum of blood colony types comparable to human ESCs (Figure 4A; Table S1). A subset of clones was further plated onto matrigel and differentiated into Tuj1-positive neurons (ectoderm) and alpha-fetoprotein-positive endodermal cells (Figure 4B; Table S1). Finally, trilineage differentiation potential was confirmed in vivo by the formation of teratomas from dH1F-, CF-, and BJ-RiPSCs, which histologically revealed cell types of the three germ layers (Figure 4C; Figure S5, Table S1).

Taken together, these data demonstrate by the most stringent criteria available to human pluripotent cells (Chan et al., 2009; Smith et al., 2009) that modified RNA-derived iPSC clones from multiple independent derivations were reprogrammed to pluripotency and closely recapitulated the functional and molecular properties of human ESCs.

Modified RNAs Generate iPSCs at Very High Efficiency

During the course of our experiments, we noted surprisingly high reprogramming efficiencies and rapid kinetics with which RiPSCs were generated. To quantify this more thoroughly, a number of reprogramming experiments were undertaken in which quantitative readout of efficiency was based on colony morphology and expression of the stringent pluripotency markers TRA-1-60 and TRA-1-81 (Chan et al., 2009; Lowry et al., 2008). In one set of experiments, BJ fibroblasts transfected with a five-factor modified RNA cocktail (KMOSL) demonstrated an iPSC conversion efficiency of more than 2%, regardless of whether the cells were passaged in the presence or absence of Rho-associated kinase (ROCK), Y-27632 (Figures 5A and 5B; Table 1). This efficiency was two orders of magnitude higher than those typically reported for virus-based derivations. Moreover, in contrast to virus-mediated BJ-iPSC derivations, in which iPSC colonies typically take around 4 weeks to emerge, by day 17 of RNA transfection the plates had already become overgrown with ESC-like colonies (Figure 5A).

We next evaluated the contributions of low-oxygen culture and LIN28 to the efficiency of RiPSC derivation. The yield of TRA-1-60/TRA-1-81-positive colonies in the ambient (20%) oxygen condition was 4-fold lower than in the cultures maintained at 5% O_2 when using KMOS RNA, but this deficit was negated when LIN28 was added to the cocktail (Figures 5C and 5D; Table 1). The highest conversion efficiency (4.4%) was observed when low-oxygen culture and the five-factor KMOSL cocktail were combined.

To directly compare the kinetics and efficiency of our RiPSC derivation protocol against an established viral protocol, we conducted an experiment in which dH1f fibroblasts were transfected with either KMOS-modified RNAs or transduced with KMOS retroviruses in parallel. As had been observed in previous experiments, ESC-like colonies began to emerge toward the end of the second week on the RNA-transfected cultures, and the plates became overgrown with ESC-like colonies by the 16th and final day of transfection. By contrast, no ESC-like colonies had appeared in the retrovirally transduced cultures by this time point, and colonies began to emerge only on the 24th day post-transduction, a time point consistent with previous reports describing iPSC derivation by retroviruses (Lowry et al., 2008; Takahashi et al., 2007). The retroviral cultures were fixed for analysis on day 32. Both arms of the experiment were then immunostained for TRA-1-60 and colonies were counted. iPSC derivation efficiencies were 1.4% and 0.04% for modified RNA and retrovirus, respectively, corresponding to 36-fold higher conversion efficiency with the modified RNA protocol (Figures 5E and 5F; Table 1). These experiments also revealed that the

Please cite this article in press as: Warren et al., Highly Efficient Reprogramming to Pluripotency and Directed Differentiation of Human Cells with Synthetic Modified mRNA, Cell Stem Cell (2010), doi:10.1016/j.stem.2010.08.012

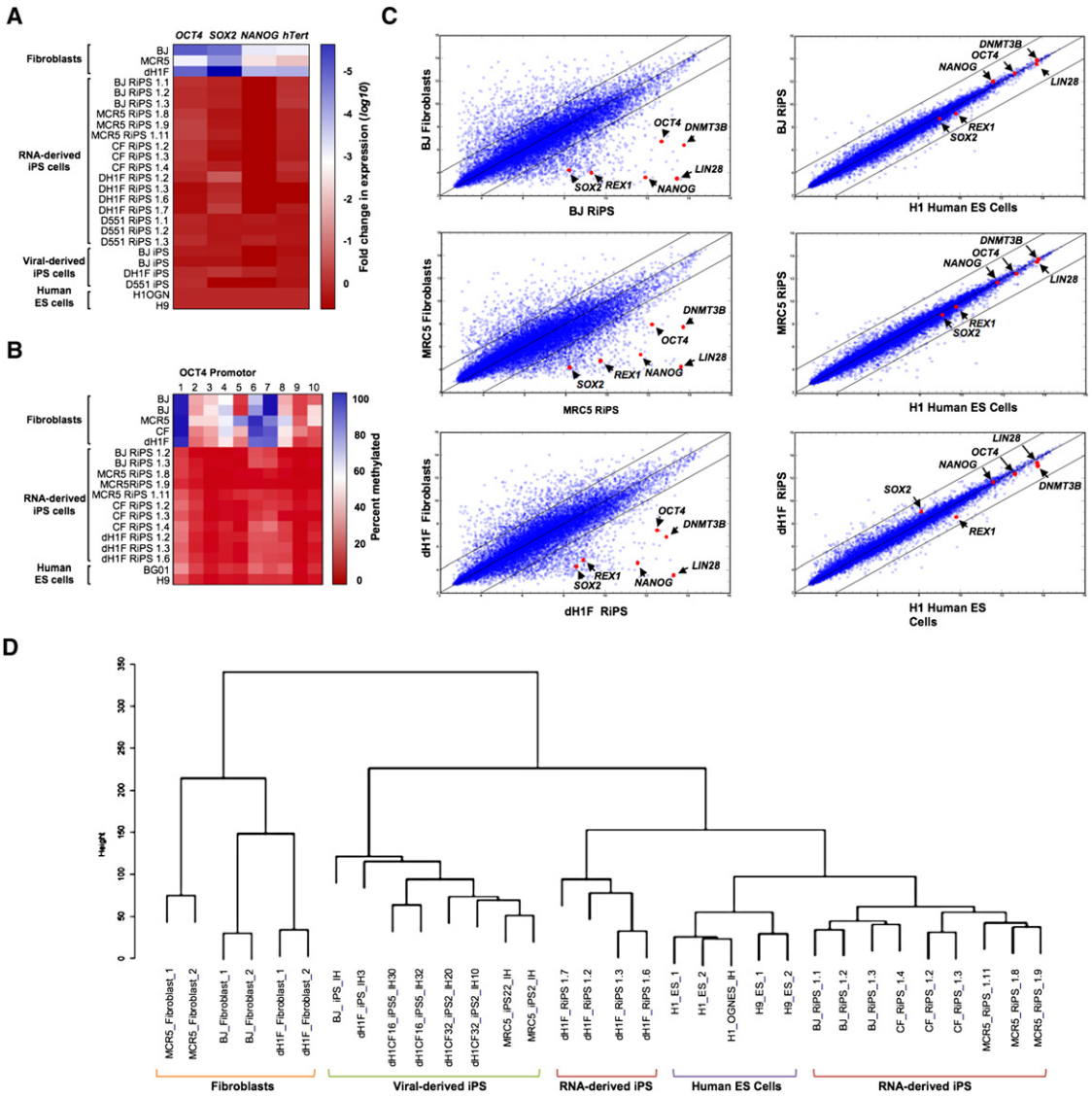

Figure 3. Molecular Characterization of RiPSCs

(A) Heatmap showing results of qRT-PCR analysis measuring the expression of pluripotency-associated genes in RiPSC lines, parental fibroblasts, and viral-derived iPSCs relative to hESC controls.

(B) Heatmap showing results of OCT4 promoter methylation analysis of RiPSC lines, parental fibroblasts, and hESC controls.

(C) Global gene expression profiles of BJ-, MRC5-, and dH1F-derived RiPSCs shown in scatter plots against parental fibroblasts and hESCs with pluripotency-associated transcripts indicated.

(D) Dendrogram showing unsupervised hierarchical clustering of the global expression profiles for RiPSCs, parental fibroblasts, hESCs, and virus-derived iPSCs.

kinetics of modified RNA iPSC derivation were almost twice as fast as retroviral iPSC derivation. Thus, by the combined criteria of colony numbers and kinetics of reprogramming, the efficiency of modified RNA iPSC derivation greatly exceeds that of conventional retroviral approaches.

It should be noted that in the experiments described above, transfected fibroblast cultures were passaged once at an early time point (day 6 or 7) in order to promote fibroblast proliferation, which has been shown to facilitate reprogramming (Hanna et al., 2009). However, in preliminary experiments, RiPSCs were also efficiently derived from BJ and Detroit 551 fibroblasts in the absence of cell passaging, indicating that splitting the culture during the reprogramming process was not required for modified RNA iPSC derivation (Figure S4, and data not shown).

Utilization of Modified RNA to Direct Differentiation of Pluripotent RiPSCs to a Terminally Differentiated Cell Fate

To realize the promise of iPSC technology for regenerative medicine or disease modeling, it is imperative that the multilineage differentiation potential of pluripotent cells be harnessed. Although progress has been made in directing the differentiation of pluripotent ESCs to various lineages by modulating the extracellular cytokine milieu, such protocols remain relatively

Please cite this article in press as: Warren et al., Highly Efficient Reprogramming to Pluripotency and Directed Differentiation of Human Cells with Synthetic Modified mRNA, Cell Stem Cell (2010), doi:10.1016/j.stem.2010.08.012

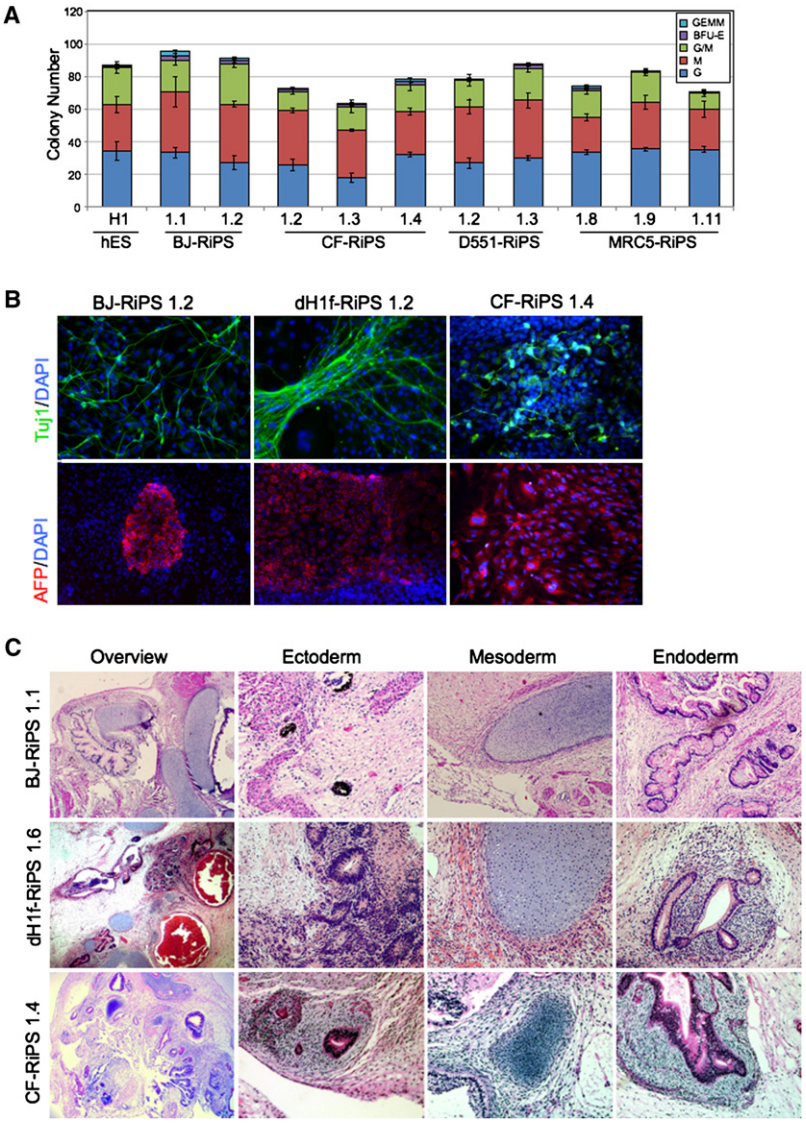

Figure 4. Trilineage Differentiation of RiPSCs

(A) Yield and typology of blood-lineage colonies produced by directed differentiation of embryoid bodies in methylcellulose assays with RiPSC clones derived from BJ, CF, D551, and MCR5 fibroblasts, and a human ESC (H1) control.

(B) Immunostaining showing expression of the lineage markers Tuj1 (neuronal, ectodermal) and alpha-fetoprotein (epithelial, endodermal) in RiPSC clones from three independent RiPSC derivations subjected to directed differentiation.

(C) Hematoxylin and eosin staining of BJ-, CF-, and dH1F-RiPSC-derived teratomas showing histological overview, ectoderm (pigmented epithelia [BJ and CF], neural rosettes [dH1F]), mesoderm (cartilage, all), and endoderm (gut-like endothelium, all). For blood formation and methylcellulose assays, n = 3 for each clone.

See also Figure S5.

inefficient. Given the high efficiency of iPSC derivation by modified RNAs, we reasoned that this technology might also be utilized to redirect pluripotent cells toward differentiated cell fates. To test this hypothesis, we subjected one of our validated RiPSC lines to a simple in vitro differentiation protocol in which FGF was withdrawn, serum added, and the cells plated onto gelatin (Figure 6). Cells obtained under these conditions were then subjected to three consecutive days of transfection with a MYOD-encoding modified RNA followed by an additional 3 days of culture in low serum conditions. The cultures were then fixed and immunostained for the myogenic markers myogenin and MyHC, which revealed a high percentage of large multinucleated myogenin and MyHC double-positive myotubes (Figure 6).

Taken together, these experiments provide proof of principle that modified RNAs can be used to both efficiently reprogram cells to a pluripotent state and direct the fate of such cells to a terminally differentiated somatic cell type.

DISCUSSION

By using a combination of RNA modifications and a soluble interferon inhibitor to overcome innate antiviral responses, we have developed a technology that enables highly efficient reprogramming of somatic cells to pluripotency and can also be harnessed to direct the differentiation of pluripotent cells toward a desired lineage. Although it is relatively technically complex, the methodology described here offers several key advantages over established reprogramming techniques. By obviating the need to perform experiments under the stringent biological containment required for virus-based approaches, modified RNA technology should make reprogramming accessible to a wider community of researchers. More fundamentally, because our technology is RNA based, it completely eliminates the risk of genomic integration and insertional mutagenesis inherent to all DNA-based methodologies, including those that are ostensibly nonintegrating. Moreover, our approach allows protein stoichiometry to be exquisitely regulated within cultures while avoiding the stochastic variation of expression typical of integrating vectors, as well as the uncontrollable effects of viral silencing. Given the stepwise character of the phenotypic changes observed during pluripotency induction (Chan et al., 2009; Smith et al., 2010), it seems likely that individual transcription factors play distinct, stage-specific roles during reprogramming. The unprecedented potential for temporal control over individual factor expression afforded by our technology should help researchers unravel these nuances, yielding insights that can be applied to further enhance the efficiency and kinetics of reprogramming.

The risk of mutagenesis is not the only safety concern holding back clinical application of induced pluripotency, and it has become increasingly apparent that all iPSCs are not created equal with respect to epigenetic landscape and developmental plasticity (Hu et al., 2010; Miura et al., 2009). In this regard, we

Please cite this article in press as: Warren et al., Highly Efficient Reprogramming to Pluripotency and Directed Differentiation of Human Cells with Synthetic Modified mRNA, Cell Stem Cell (2010), doi:10.1016/j.stem.2010.08.012

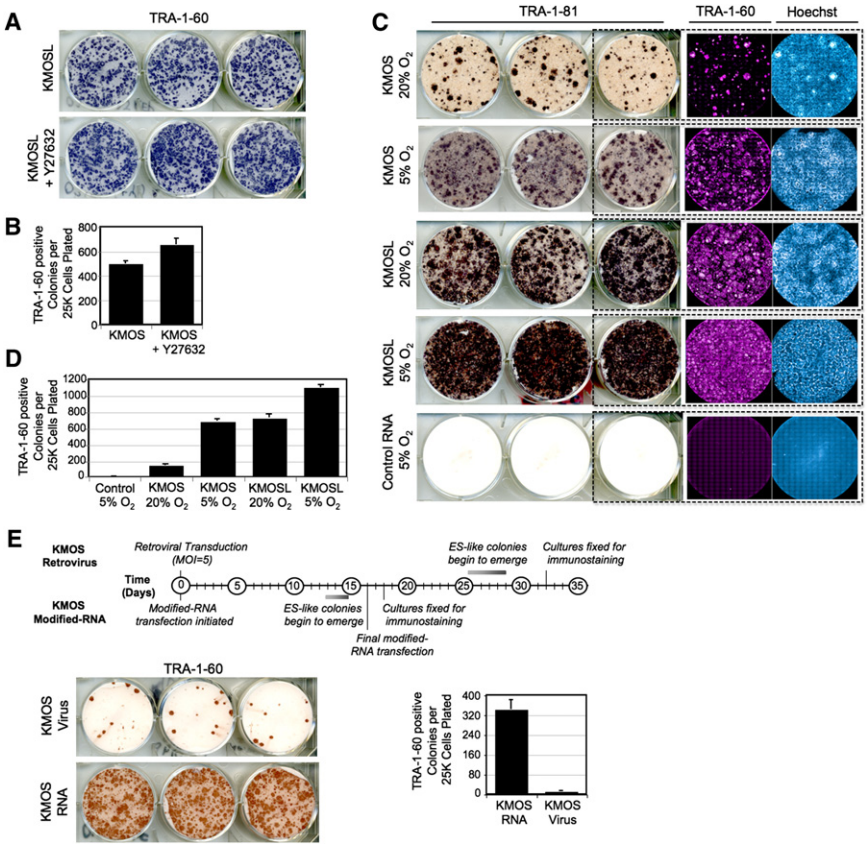

Figure 5. Pluripotency Induction by Modified RNAs Is Highly Efficient

(A and B) TRA-1-60 horseradish peroxidase (HRP) staining conducted at day 18 of a BJ-RiPSC derivation with modified RNAs encoding KMOSL (A) and frequency of TRA-1-60-positive colonies produced in the experiment relative to number of cells initially seeded (B). Error bars show SD, n = 6 for each condition.

(C and D) TRA-181 HRP, TRA-160 immunofluorescence, and Hoechst staining (C) and colony frequencies for dH1f-RiPS experiments done with 4-factor (KMOS) and 5-factor (KMOSL) modified RNA cocktails under 5% O_2 or ambient oxygen culture conditions quantified at day 18 (D). Control wells were transfected with equal doses of modified RNA encoding GFP.

(E) Kinetics and efficiency of retroviral and modified RNA reprogramming. Timeline of colony formation (top), TRA-1-60 HRP immunostaining (bottom left), and TRA-1-60-positive colony counts (bottom right) of dH1f cells reprogrammed with KMOS retroviruses (MOI = 5 of each) or modified RNA KMOS cocktails (n = 3 for each condition).

See also Figure S4.

have applied the most stringent molecular and functional criteria for reprogramming human cells to pluripotency (Chan et al., 2009; Smith et al., 2009). Our results demonstrate that modified RNA-derived iPSC clones from multiple independent derivations were fully reprogrammed to pluripotency and that the resulting cells very closely recapitulated the functional and molecular properties of human ESCs. Our observation that modified RNA-derived iPSCs more faithfully recapitulated the global transcriptional signature of human ESCs than retrovirally derived iPSCs is important because it suggests that RNA reprogramming may produce higher-quality iPSCs, possibly owing to the fact that they are transgene free.

The transient and nonmutagenic character of RNA-based protein expression could also deliver important clinical benefits outside the domain of lineage reprogramming. Indeed, the use of RNA transfection to express cancer or pathogen antigens for immunotherapy is already an active research area (Rabinovich et al., 2006, 2008; Van den Bosch et al., 2006; Weissman et al., 2000), and such approaches may benefit from the nonimmunogenic properties of modified RNAs. One can readily envisage employing modified RNA to transiently express surface proteins such as homing receptors to target cellular therapies toward specific organs, tissues, or diseased cells.

For tissue engineering to progress further into the clinic, there is a pressing need for safe and efficient means to redirect cell fate. This is doubly apparent when one considers that iPSCs are only a starting point for patient-specific therapies, and specification of clinically useful cell types is still required to produce autologous tissues for transplantation or for disease modeling. Importantly, we have demonstrated that our modified RNA-based technology enables highly efficient reprogramming and that it can equally be applied to efficiently redirect pluripotent cell fate to terminally differentiated fates without compromising genomic integrity. In light of these considerations, we believe that our approach has the potential to become a major enabling technology for cell-based therapies and regenerative medicine.

EXPERIMENTAL PROCEDURES

Construction of IVT Templates

The pipeline for production of IVT template constructs and subsequent RNA synthesis is schematized in Figure S1. The oligonucleotide sequences used in the construction of IVT templates are shown in Table S2. All oligos were synthesized by Integrated DNA Technologies (Coralville, IA). ORF PCRs were templated from plasmids bearing human KLF4, c-MYC, OCT4, SOX2, human ESC cDNA (LIN28), Clontech pIRES-eGFP (eGFP), pRVGP (d2eGFP), and CMV-MyoD from Addgene. The ORF of the low-stability nuclear GFP was constructed by combining the d2eGFP ORF with a 3′ nuclear localization sequence. PCR reactions were performed with HiFi Hotstart (KAPA Biosystems, Woburn, MA) per the manufacturer's instructions. Splint-mediated ligations were carried out with Ampligase Thermostable DNA Ligase (Epicenter Biotechnologies, Madison, WI). UTR ligations were conducted in the presence of 200 nM UTR oligos and 100 nM splint oligos, with 5 cycles of the following annealing profile: 95°C for 10 s; 45°C for 1 min; 50°C for 1 min; 55°C for 1 min; 60°C for 1 min. A phosphorylated forward primer was employed in the ORF PCRs to facilitate ligation of the top strand to the 5′ UTR fragment. The 3′ UTR fragment was also 5′-phosphorylated via polynucleotide kinase (New England Biolabs, Ipswich, MA). All intermediate PCR and ligation products were purified with QIAquick spin columns (QIAGEN, Valencia, CA) before further processing. Template PCR amplicons were subcloned with the pcDNA

Please cite this article in press as: Warren et al., Highly Efficient Reprogramming to Pluripotency and Directed Differentiation of Human Cells with Synthetic Modified mRNA, Cell Stem Cell (2010), doi:10.1016/j.stem.2010.08.012

Table 1. Quantification of Reprogramming Efficiency

Experiment	Cells Plated	Split	Condition	Well Fraction	Colonies/Well	Efficiency (%)
BJ (KMOSL)	300,000	d7	Y27632-	1/24	249 ± 21	2.0
			Y27632+	1/24	326 ± 49	2.6
4-Factor (KMOS) versus 5-Factor (KMOSL)	50,000	d6	4F 20% O_2	1/6	48 ± 18	0.6
			4F 5% O_2	1/6	228 ± 30	2.7
			5F 20% O_2	1/6	243 ± 42	2.9
			5F 5% O_2	1/6	367 ± 38	4.4
RNA versus Virus (KMOS)	100,000	d6	virus	1/3	13 ± 3.5	0.04
			RNA	1/6	229 ± 39	1.4

For each experimental condition, efficiency was calculated by dividing the average count of TRA-1-60-positive colonies per well by the initial number of cells plated, scaled to the fraction of cells replated in each well. Cultures were passaged at day 6 or 7 as indicated. The BJ experiment was started in a 10 cm dish; dH1f trials in individual wells of a 6-well plate. Colony counts are shown ± SD, n = 6, except in the RNA versus Virus trial, where n = 9 for virus, n = 18 for RNA.

3.3-TOPO TA cloning kit (Invitrogen, Carlsbad, CA). Plasmid inserts were excised by restriction digest and recovered with SizeSelect gels (Invitrogen) before being used to template tail PCRs.

Synthesis of Modified RNA

RNA was synthesized with the MEGAscript T7 kit (Ambion, Austin, TX), with 1.6 μg of purified tail PCR product to template each 40 μL reaction. A custom ribonucleoside blend was used comprising 3′-0-Me-m^{7}G(5′)ppp(5′)G ARCA cap analog (New England Biolabs), adenosine triphosphate and guanosine triphosphate (USB, Cleveland, OH), 5-methylcytidine triphosphate and pseudouridine triphosphate (TriLink Biotechnologies, San Diego, CA). Final nucleotide reaction concentrations were 6 mM for the cap analog, 1.5 mM for guanosine triphosphate, and 7.5 mM for the other nucleotides. Reactions were incubated 3–6 hr at 37°C and DNase treated as directed by the manufacturer. RNA was purified with Ambion MEGAclear spin columns, then treated with Antarctic Phosphatase (New England Biolabs) for 30 min at 37°C to remove residual 5′-triphosphates. Treated RNA was repurified, quantitated by Nanodrop (Thermo Scientific, Waltham, MA), and adjusted to 100 ng/μL working concentration by addition of Tris-EDTA (pH 7.0). RNA reprogramming cocktails were prepared by pooling individual 100 ng/μL RNA stocks to produce a 100 ng/μL (total) blend. The KMOS[L]+GFP cocktails were formulated to give equal molarity for each component except for OCT4, which was included at 3× molar concentration. Volumetric ratios used for pooling were as follows: 170:160:420:130:120[:90] (KLF4:c-MYC:OCT4:SOX2:GFP[:LIN28]).

Cells

Primary human neonatal epidermal keratinocytes, BJ human neonatal foreskin fibroblasts, MRC-5 human fetal lung fibroblasts, and Detroit 551 human fetal skin fibroblasts were obtained from ATCC (Manassas, VA). CF cells were obtained with informed consent from a skin biopsy taken from an adult cystic fibrosis patient. dH1f fibroblasts were subcloned from fibroblasts produced by directed differentiation of the H1-OGN human ESC line as previously described (Park et al., 2008). BGO1 hESCs were obtained from BresaGen (Athens, GA). H1 and H9 hESCs were obtained from WiCell (Madison, Wi).

RNA Transfection

RNA transfections were carried out with RNAiMAX (Invitrogen) or TransIT-mRNA (Mirus Bio, Madison, WI) cationic lipid delivery vehicles. RNAiMAX was used for RiPSC derivations, the RiPSC-to-myogenic conversion, and for the multiple cell type transfection experiment documented in Figure S2. All other transfections were performed with TransIT-mRNA. For RNAiMAX transfections, RNA and reagent were first diluted in Opti-MEM basal media (Invitrogen). 100 ng/μL RNA was diluted 5× and 5 μL of RNAiMAX per microgram of RNA was diluted 10×, then these components were pooled and incubated 15 min at room temperature (RT) before being dispensed to culture

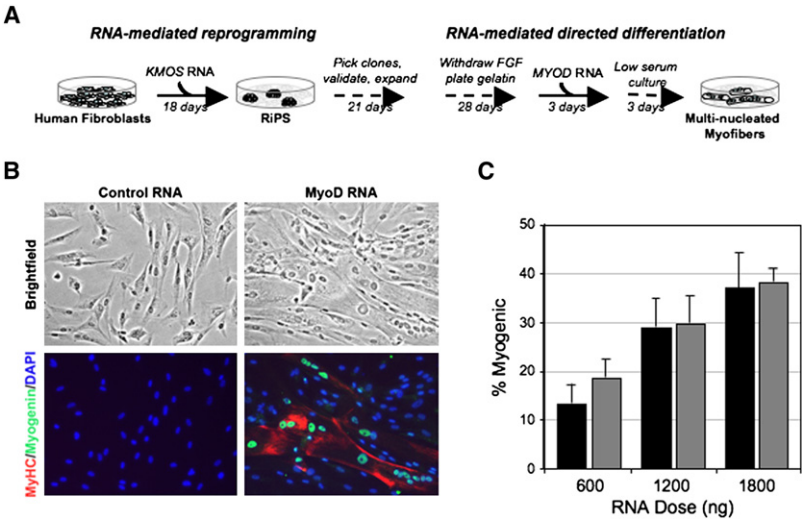

Figure 6. Efficient Directed Differentiation of RiPSCs to Terminally Differentiated Myogenic Fate via Modified RNA

(A) Schematic of experimental design.

(B) Bright-field and immunostained images showing large, multinucleated, myosin heavy chain (MyHC) and myogenin-positive myotubes in cells fixed 3 days after cessation of *MYOD* modified RNA transfection. Modified RNA encoding GFP was administered to the controls.

(C) Penetrance of myogenic conversion relative to daily RNA dose. Black bars refer to an experiment in which cultures were plated at 10^4 cells/cm^2, gray bars to cultures plated at 5 × 10^3 cells/cm^2. Error bars show SD for triplicate wells.

media. For TransIT-mRNA transfections, 100 ng/μL RNA was diluted 10× in Opti-MEM and BOOST reagent was added (2 μL per microgram of RNA), then TransIT-mRNA was added (2 μL per microgram of RNA), and the RNA-lipid complexes were delivered to culture media after a 2 min incubation at RT. RNA transfections were performed in Nutristem xeno-free hESC media (Stemgent, Cambridge, MA) for RiPSC derivations, Dermal Cell Basal Medium plus Keratinocyte Growth Kit (ATCC) for keratinocyte experiments, and Opti-MEM plus 2% FBS for all other experiments described. The B18R interferon inhibitor (eBioscience, San Diego, CA) was used as a media supplement at 200 ng/mL.

qRT-PCR

Transfected cells were lysed with 400 μL CellsDirect reagents (Invitrogen), and 20 μL of each lysate was taken forward to a 50 μL reverse transcription reaction via the VILO cDNA synthesis kit (Invitrogen). Reactions were purified on QIAquick columns (QIAGEN). qRT-PCR reactions were performed with SYBR FAST qPCR supermix (KAPA Biosystems).

Reprogramming to Pluripotency

Gamma-irradiated human neonatal fibroblast feeders (GlobalStem, Rockville, MD) were seeded at 33,000 cells/cm^2. Nutristem media was replaced daily, 4 hr after transfection, and supplemented with 100 ng/mL bFGF and 200 ng/mL B18R (eBioscience, San Diego, CA). Where applied, VPA was added to media at 1 mM final concentration on days 8–15 of reprogramming. Low-oxygen experiments were carried out in a NAPCO 8000 WJ incubator (Thermo Scientific). Media were equilibrated at 5% O_2 for approximately 4 hr before use. Cultures were passaged with TrypLE Select recombinant protease (Invitrogen). Y27632 ROCK inhibitor (Watanabe et al., 2007) was used at 10 μM in recipient plates until the next media change. The daily RNA dose applied in the RiPSC derivations was 1200 ng per well (6-well plate format) or 8 μg to a 10 cm dish.

For RNA versus retrovirus experiments, starting cultures were seeded with 100,000 cells in individual wells of a 6-well plate via fibroblast media (DMEM+10% FBS). The next day (day 1), KMOS RNA transfections were initiated in the RNA plate, and the viral plate was transduced with a KMOS retroviral cocktail (MOI = 5 for each virus). All wells were passaged on day 6, with split ratios of 1:6 for the RNA wells and 1:3 for the virus wells. The conditions applied in the RNA arm of the trial were as in the initial RiPSC derivation, including the use of Nutristem supplemented with 100 ng/mL bFGF, 5% O_2 culture, and human fibroblast feeders. Ambient oxygen tension and other conventional iPSC derivation conditions were used in the viral arm, the cells being grown in fibroblast media without feeders until the day 6 split, then being replated onto CF1 MEF feeders (GlobalStem) with a switch to hESC media based on Knockout Serum Replacement (Invitrogen) supplemented with 10 ng/mL bFGF.

RiPSC Culturing

RiPSC colonies were mechanically picked and transferred to MEF-coated 24-well plates with standard hESC medium containing 5 μM Y27632 (BioMol, Plymouth Meeting, PA). The hESC media comprised DMEM/F12 supplemented with 20% Knockout Serum Replacement (Invitrogen), 10 ng/mL of bFGF (Gembio, West Sacramento, CA), 1× nonessential amino acids (Invitrogen), 0.1 mM β-ME (Sigma), 1 mM L-glutamine (Invitrogen), plus antibiotics. Clones were mechanically passaged once more to MEF-coated 6-well plates, and then expanded via enzymatic passaging with collagenase IV (Invitrogen). For RNA and DNA preparation, cells were plated onto hESC-qualified Matrigel (BD Biosciences) in mTeSR (Stem Cell Technologies, Vancouver, BC) and further expanded by enzymatic passaging with dispase (Stem Cell Technologies).

Immunostaining

Cells were fixed in 4% paraformaldehyde for 20 min. Washed cells were treated with 0.2% Triton X (Sigma) in PBS for 30 min. Cells were blocked with 3% BSA (Invitrogen) and 5% donkey serum (Sigma) for 2 hr at RT. Cells were stained in blocking buffer with primary antibodies at 4°C overnight. Cells were washed and stained with secondary antibodies and 1 μg/mL Hoechst 33342 (Invitrogen) in blocking buffer for 3 hr at 4°C or for 1 hr at RT, protected from light. Antibodies were used, at 1:100 dilution: TRA-1-60-Alexa Fluor 647, TRA-1-81-Alexa Fluor 488, SSEA-4-Alexa Fluor 647, and SSEA-3-Alexa 488 (BD Biosciences). Primary OCT4 and NANOG antibodies (Abcam, Cambridge, MA) were used at 0.5 μg/mL, and an anti-rabbit IgG Alexa Fluor 555 (Invitrogen) was used as the secondary. Images were acquired with a Pathway 435 bioimager (BD Biosciences). Live imaging was performed as described previously (Chan et al., 2009). For pluripotency factor time course experiments, transfected human keratinocytes were trypsinized, washed with PBS, and fixed in 4% paraformaldehyde for 10 min. Fixed cells were washed with 0.1 M glycine, then blocked and permeabilized in PBS/0.5% saponin/1% goat serum (Rockland Immunochemicals, Gilbertsville, PA) for 20 min. Cells were incubated for 1 hr at RT with 1:100 diluted primary antibodies for KLF4, OCT4, and SOX2 (Stemgent), washed, then for 45 min at RT with 1:200-diluted DyLight 488-labeled secondary antibodies (goat anti-mouse IgG+IgM and goat anti-rabbit IgG). Cells were suspended in PBS and analyzed by flow cytometry.

Gene Expression Analysis

RNA was isolated with the RNeasy kit (QIAGEN) according to the manufacturer's instructions. First-strand cDNA was primed with oligo(dT) primers and qPCR was performed with primer sets as described previously (Park et al., 2008), with Brilliant SYBR Green master mix (Stratagene, La Jolla, CA). For the microarray analysis, RNA probes were prepared and hybridized to Human Genome U133 Plus 2.0 oligonucleotide microarrays (Affymetrix, Santa Clara, CA) per the manufacturer's instructions. Arrays were processed by the Coriell Institute Genotyping and Microarray Center (Camden, NJ). Gene expression levels were normalized with the Robust Multichip Average (RMA) algorithm. Hierarchical clustering was performed by means of the Euclidean distance with average linkage method. The similarity metric for comparison between different cell lines is indicated on the height of cluster dendrogram.

Bisulfite Sequencing

DNA was extracted with the DNeasy Blood and Tissue kit (QIAGEN) according to the manufacturer's protocol. Bisulfite treatment of genomic DNA was carried out with EZ DNA Methylation Kit (Zymo Research, Orange, CA) according to the manufacturer's protocol. For pyrosequencing analysis, the bisulfate-treated DNA was first amplified by HotStar Taq Polymerase (QIAGEN) for 45 cycles of (95°C 30 s; 53°C 30 s; 72°C 30 s). The analysis was performed by EpigenDx with the PSQ96HS system according to standard procedures with primers that were developed by EpigenDx for the CpG sites at positions (−50) to (+96) from the start codon of the *OCT4* gene.

Trilineage Differentiation

Embryoid body (EB) hematopoietic differentiation was performed as previously described (Chadwick et al., 2003). In brief, RiPSCs and hESC controls were passaged with collagenase IV and transferred (3:1) in differentiation medium to 6-well low-attachment plates and placed on a shaker in a 37°C incubator overnight. Starting the next day, media was supplemented with the following hematopoietic cytokines: 10 ng/mL of interleukin-3 (R&D Systems, Minneapolis, MN) and interleukin-6 (R&D), 50 ng/mL of G-CSF (Amgen, Thousand Oaks, CA) and BMP-4 (R&D), and 300 ng/mL of SCF (Amgen) and Flt-3 (R&D). Media was changed every 3 days. On day 14 of differentiation, EBs were dissociated with collagenase B (Roche, Indianapolis, IN). 2 × 10^4 differentiated cells were plated into methylcellulose H4434 (Stem Cell Technologies) and transferred with a blunt needle onto 35 mm dishes (Stem Cell Technologies) in triplicate and incubated at 37°C and 5% CO_2 for 14 days. Colony forming units (CFUs) were scored based on morphological characteristics.

For neuronal differentiation, cells were differentiated at 70% confluency as a monolayer in neuronal differentiation medium (DMEM/F12, Glutamax 1%, B27-Supplement 1%, N2-Supplement 2%, P/S 1%, and noggin 20 ng/ml). After 7 days, neuronal structures were visible. For endoderm differentiation (AFP stain), cells were differentiated as a monolayer in endoderm differentiation medium (DMEM, B27(-RA), and 100 ng/ml activin-a) for 7 days, then switched to growth medium (DMEM, 10% FBS, 1% P/S) and continued differentiation for 7 days. Antibodies used were as follows: anti-β-Tubulin III (Tuj1) rabbit anti-human (Sigma, St. Louis, MO), 1:500; AFP (h-140) rabbit polyclonal IgG (Santa Cruz Biotechnology, Santa Cruz, CA), 1:100 dilution. Secondary antibodies were conjugated to Alexa Fluor 488 or Alexa Fluor 594.

For cardiomyocyte differentiation, colonies were digested at 70% confluency with dispase and placed in suspension culture for embryoid body (EB) formation in differentiation medium (DMEM, 15% FBS, 100 μM ascorbic acid). After 11 days, EBs were plated to adherent conditions via gelatin and the same medium. Beating cardiomyocytes were observed 3 days after replating.

For teratomas, 2.5 × 10^6 cells were spun down, and all excess media was removed. In 20-week-old female SCID mice, the capsule of the right kidney was gently elevated, and one droplet of concentrated cells was inserted under the capsule. Tumors harvested at 6–12 weeks were fixed in 4% PFA, run through an ethanol gradient, and stored in 70% ethanol. Specimens were sectioned and stained with H&E.

Myogenic Differentiation of RiPSCs

Validated RiPSCs were plated into wells coated with 0.1% gelatin (Millipore, Billerica, MA) and cultured in DMEM+10% FBS for 4 weeks with passaging every 4–6 days via trypsin. The culture media was switched to Opti-MEM+2% FBS, and the cells were transfected with modified RNA encoding either murine MYOD or GFP the following day, and for the following 2 days. Media was supplemented with B18R and replaced 4 hr after each transfection. After the third and final transfection, the media was switched to DMEM+3% horse serum, and cultures were incubated for a further 3 days. Cells were then fixed in 4% PFA and immunostained as previously described (Shea et al., 2010). The percentage of myogenin-positive nuclei/total nuclei and nuclei/MyHC-positive myotubes was quantified, with a minimum of 500 nuclei counted per condition.

Technical Notes

Although reprogramming and directed differentiation via modified RNAs are efficient processes, the protocols involved are nonetheless multistepped and complex. It is therefore advised that in efforts to apply this methodology, all steps of the protocols described herein are followed rigorously and quality controlled. Foremost among these: templates for RNA synthesis must be sequenced, and production of in vitro transcribed modified RNAs must be quality controlled by gel electrophoresis and spectrophotometry. Critically, the expression of proteins with modified RNAs must be confirmed by immunostaining. Modified RNAs must also be tested for immunogenicity at multiple points throughout the course of the experiment. Successful daily transfection must be monitored by inclusion of modified RNA encoding a fluorescent reporter throughout the course of experiments. Any reagents involved in supporting pluripotency induction (media, feeder cells, etc.) should be tested for their ability to support the growth of pluripotent cells prior to the start of experiments. As is true of reprogramming by other methods, the quality of the starting cells (e.g., passage number) impacts reprogramming via our technology.

ACCESSION NUMBERS

The microarray data are available in the Gene Expression Omnibus (GEO) database (http://www.ncbi.nlm.nih.gov/gds) under the accession number GSE23583.

SUPPLEMENTAL INFORMATION

Supplemental Information includes five figures, three tables, and one movie and can be found with this article online at doi:10.1016/j.stem.2010.08.012.

ACKNOWLEDGMENTS

The authors wish to thank Sun Hur, Victor Li, Laurence Daheron, Odelya Hartung, Alys Peisley, Sutheera Ratanasirintrawoot, Brad Hamilton, Chenmei Luo, Jonathan Kagan, Julie Sahalie, Alejandro De Los Angeles, and Lior Zangi for help, insight, and suggestions. D.J.R., A.M., G.Q.D, A.S.B, C.C., and T.M.S. were supported by grants from the Harvard Stem Cell Institute. Y.-H.L. is supported by the A*Star Institute of Medical Biology and Singapore stem cell consortium. T.A. was supported by the Roberto and Allison Mignone Fund for Stem Cell Research. J.J.C. is supported by Howard Hughes Medical Institute, SysCODE (Systems-based Consortium for Organ Design & Engineering), and NIH grant # RL1DE019021. D.J.R. recently founded a company, ModeRNA Therapeutics, dedicated to the clinical translation of this technology. G.Q.D. is a member of the scientific advisory boards and holds equity in the following companies: Epizyme, iPierian, Solasia KK, and MPM Capital, LLP. C.C. is on the SAB of Ipierian. L.W. is a consultant for Stemgent. T.A., Y-H.L., and H.L. contributed equally to this work.

Received: March 30, 2010
Revised: May 11, 2010
Accepted: August 11, 2010
Published online: September 30, 2010

REFERENCES

Audouy, S., and Hoekstra, D. (2001). Cationic lipid-mediated transfection in vitro and in vivo (review). Mol. Membr. Biol. *18*, 129–143.

Chadwick, K., Wang, L., Li, L., Menendez, P., Murdoch, B., Rouleau, A., and Bhatia, M. (2003). Cytokines and BMP-4 promote hematopoietic differentiation of human embryonic stem cells. Blood *102*, 906–915.

Chan, E.M., Ratanasirintrawoot, S., Park, I.H., Manos, P.D., Loh, Y.H., Huo, H., Miller, J.D., Hartung, O., Rho, J., Ince, T.A., et al. (2009). Live cell imaging distinguishes bona fide human iPS cells from partially reprogrammed cells. Nat. Biotechnol. *27*, 1033–1037.

Chang, C.-W., Lai, Y.-S., Pawlik, K.M., Liu, K., Sun, C.-W., Li, C., Schoeb, T.R., and Townes, T.M. (2009). Polycistronic lentiviral vector for "hit and run" reprogramming of adult skin fibroblasts to induced pluripotent stem cells. Stem Cells *27*, 1042–1049.

Davis, R.L., Weintraub, H., and Lassar, A.B. (1987). Expression of a single transfected cDNA converts fibroblasts to myoblasts. Cell *51*, 987–1000.

Diebold, S.S., Kaisho, T., Hemmi, H., Akira, S., and Reis e Sousa, C. (2004). Innate antiviral responses by means of TLR7-mediated recognition of single-stranded RNA. Science *303*, 1529–1531.

Elango, N., Elango, S., Shivshankar, P., and Katz, M.S. (2005). Optimized transfection of mRNA transcribed from a d(A/T)100 tail-containing vector. Biochem. Biophys. Res. Commun. *330*, 958–966.

Fusaki, N., Ban, H., Nishiyama, A., Saeki, K., and Hasegawa, M. (2009). Efficient induction of transgene-free human pluripotent stem cells using a vector based on Sendai virus, an RNA virus that does not integrate into the host genome. Proc. Jpn. Acad., Ser. B, Phys. Biol. Sci. *85*, 348–362.

Hanna, J., Saha, K., Pando, B., van Zon, J., Lengner, C.J., Creyghton, M.P., van Oudenaarden, A., and Jaenisch, R. (2009). Direct cell reprogramming is a stochastic process amenable to acceleration. Nature *462*, 595–601.

Holtkamp, S., Kreiter, S., Selmi, A., Simon, P., Koslowski, M., Huber, C., Türeci, O., and Sahin, U. (2006). Modification of antigen-encoding RNA increases stability, translational efficacy, and T-cell stimulatory capacity of dendritic cells. Blood *108*, 4009–4017.

Hornung, V., Ellegast, J., Kim, S., Brzózka, K., Jung, A., Kato, H., Poeck, H., Akira, S., Conzelmann, K.-K., Schlee, M., et al. (2006). 5′-Triphosphate RNA is the ligand for RIG-I. Science *314*, 994–997.

Hu, B.Y., Weick, J.P., Yu, J., Ma, L.X., Zhang, X.Q., Thomson, J.A., and Zhang, S.C. (2010). Neural differentiation of human induced pluripotent stem cells follows developmental principles but with variable potency. Proc. Natl. Acad. Sci. USA *107*, 4335–4340.

Huangfu, D., Maehr, R., Guo, W., Eijkelenboom, A., Snitow, M., Chen, A.E., and Melton, D.A. (2008). Induction of pluripotent stem cells by defined factors is greatly improved by small-molecule compounds. Nat. Biotechnol. *26*, 795–797.

Jia, F., Wilson, K.D., Sun, N., Gupta, D.M., Huang, M., Li, Z., Panetta, N.J., Chen, Z.Y., Robbins, R.C., Kay, M.A., et al. (2010). A nonviral minicircle vector for deriving human iPS cells. Nat. Methods *7*, 197–199.

Kaji, K., Norrby, K., Paca, A., Mileikovsky, M., Mohseni, P., and Woltjen, K. (2009). Virus-free induction of pluripotency and subsequent excision of reprogramming factors. Nature *458*, 771–775.

Karikó, K., and Weissman, D. (2007). Naturally occurring nucleoside modifications suppress the immunostimulatory activity of RNA: implication for therapeutic RNA development. Curr. Opin. Drug Discov. Devel. *10*, 523–532.

Karikó, K., Buckstein, M., Ni, H., and Weissman, D. (2005). Suppression of RNA recognition by Toll-like receptors: The impact of nucleoside modification and the evolutionary origin of RNA. Immunity *23*, 165–175.

Karikó, K., Muramatsu, H., Welsh, F.A., Ludwig, J., Kato, H., Akira, S., and Weissman, D. (2008). Incorporation of pseudouridine into mRNA yields superior nonimmunogenic vector with increased translational capacity and biological stability. Mol. Ther. *16*, 1833–1840.

Kawai, T., and Akira, S. (2007). Antiviral signaling through pattern recognition receptors. J. Biochem. *141*, 137–145.

Kawamura, T., Suzuki, J., Wang, Y.V., Menendez, S., Morera, L.B., Raya, A., Wahl, G.M., and Belmonte, J.C. (2009). Linking the p53 tumour suppressor pathway to somatic cell reprogramming. Nature *460*, 1140–1144.

Kim, D., Kim, C.-H., Moon, J.-I., Chung, Y.-G., Chang, M.-Y., Han, B.-S., Ko, S., Yang, E., Cha, K.Y., Lanza, R., and Kim, K.S. (2009). Generation of human induced pluripotent stem cells by direct delivery of reprogramming proteins. Cell Stem Cell *4*, 472–476.

Li, X., Zhao, X., Fang, Y., Jiang, X., Duong, T., Fan, C., Huang, C.-C., and Kain, S.R. (1998). Generation of destabilized green fluorescent protein as a transcription reporter. J. Biol. Chem. *273*, 34970–34975.

Lowry, W.E., Richter, L., Yachechko, R., Pyle, A.D., Tchieu, J., Sridharan, R., Clark, A.T., and Plath, K. (2008). Generation of human induced pluripotent stem cells from dermal fibroblasts. Proc. Natl. Acad. Sci. USA *105*, 2883–2888.

Miura, K., Okada, Y., Aoi, T., Okada, A., Takahashi, K., Okita, K., Nakagawa, M., Koyanagi, M., Tanabe, K., Ohnuki, M., et al. (2009). Variation in the safety of induced pluripotent stem cell lines. Nat. Biotechnol. *27*, 743–745.

Nallagatla, S.R., and Bevilacqua, P.C. (2008). Nucleoside modifications modulate activation of the protein kinase PKR in an RNA structure-specific manner. RNA *14*, 1201–1213.

Nallagatla, S.R., Toroney, R., and Bevilacqua, P.C. (2008). A brilliant disguise for self RNA: 5′-end and internal modifications of primary transcripts suppress elements of innate immunity. RNA Biol. *5*, 140–144.

Okita, K., Nakagawa, M., Hyenjong, H., Ichisaka, T., and Yamanaka, S. (2008). Generation of mouse induced pluripotent stem cells without viral vectors. Science *322*, 949–953.

Papapetrou, E.P., Tomishima, M.J., Chambers, S.M., Mica, Y., Reed, E., Menon, J., Tabar, V., Mo, Q., Studer, L., and Sadelain, M. (2009). Stoichiometric and temporal requirements of Oct4, Sox2, Klf4, and c-Myc expression for efficient human iPSC induction and differentiation. Proc. Natl. Acad. Sci. USA *106*, 12759–12764.

Park, I.-H., Zhao, R., West, J.A., Yabuuchi, A., Huo, H., Ince, T.A., Lerou, P.H., Lensch, M.W., and Daley, G.Q. (2008). Reprogramming of human somatic cells to pluripotency with defined factors. Nature *451*, 141–146.

Pichlmair, A., Schulz, O., Tan, C.P., Näslund, T.I., Liljeström, P., Weber, F., and Reis e Sousa, C. (2006). RIG-I-mediated antiviral responses to single-stranded RNA bearing 5′-phosphates. Science *314*, 997–1001.

Rabinovich, P.M., Komarovskaya, M.E., Ye, Z.J., Imai, C., Campana, D., Bahceci, E., and Weissman, S.M. (2006). Synthetic messenger RNA as a tool for gene therapy. Hum. Gene Ther. *17*, 1027–1035.

Rabinovich, P.M., Komarovskaya, M.E., Wrzesinski, S.H., Alderman, J.L., Budak-Alpdogan, T., Karpikov, A., Guo, H., Flavell, R.A., Cheung, N.K., Weissman, S.M., and Bahceci, E. (2008). Chimeric receptor mRNA transfection as a tool to generate antineoplastic lymphocytes. Hum. Gene Ther. *20*, 51–61.

Randall, R.E., and Goodbourn, S. (2008). Interferons and viruses: An interplay between induction, signalling, antiviral responses and virus countermeasures. J. Gen. Virol. *89*, 1–47.

Shea, K.L., Xiang, W., LaPorta, V.S., Licht, J.D., Keller, C., Basson, M.A., and Brack, A.S. (2010). Sprouty1 regulates reversible quiescence of a self-renewing adult muscle stem cell pool during regeneration. Cell Stem Cell *6*, 117–129.

Smith, K.P., Luong, M.X., and Stein, G.S. (2009). Pluripotency: Toward a gold standard for human ES and iPS cells. J. Cell. Physiol. *220*, 21–29.

Smith, Z.D., Nachman, I., Regev, A., and Meissner, A. (2010). Dynamic single-cell imaging of direct reprogramming reveals an early specifying event. Nat. Biotechnol. *28*, 521–526.

Stadtfeld, M., Nagaya, M., Utikal, J., Weir, G., and Hochedlinger, K. (2008). Induced pluripotent stem cells generated without viral integration. Science *322*, 945–949.

Symons, J.A., Alcamí, A., and Smith, G.L. (1995). Vaccinia virus encodes a soluble type I interferon receptor of novel structure and broad species specificity. Cell *81*, 551–560.

Takahashi, K., and Yamanaka, S. (2006). Induction of pluripotent stem cells from mouse embryonic and adult fibroblast cultures by defined factors. Cell *126*, 663–676.

Takahashi, K., Tanabe, K., Ohnuki, M., Narita, M., Ichisaka, T., Tomoda, K., and Yamanaka, S. (2007). Induction of pluripotent stem cells from adult human fibroblasts by defined factors. Cell *131*, 861–872.

Uematsu, S., and Akira, S. (2007). Toll-like receptors and Type I interferons. J. Biol. Chem. *282*, 15319–15323.

Utikal, J., Polo, J.M., Stadtfeld, M., Maherali, N., Kulalert, W., Walsh, R.M., Khalil, A., Rheinwald, J.G., and Hochedlinger, K. (2009). Immortalization eliminates a roadblock during cellular reprogramming into iPS cells. Nature *460*, 1145–1148.

Uzri, D., and Gehrke, L. (2009). Nucleotide sequences and modifications that determine RIG-I/RNA binding and signaling activities. J. Virol. *83*, 4174–4184.

Van den Bosch, G.A., Van Gulck, E., Ponsaerts, P., Nijs, G., Lenjou, M., Apers, L., Kint, I., Heyndrickx, L., Vanham, G., Van Bockstaele, D.R., et al. (2006). Simultaneous activation of viral antigen-specific memory CD4+ and CD8+ T-cells using mRNA-electroporated CD40-activated autologous B-cells. J. Immunother. *29*, 512–523.

Van Tendeloo, V.F., Ponsaerts, P., Lardon, F., Nijs, G., Lenjou, M., Van Broeckhoven, C., Van Bockstaele, D.R., and Berneman, Z.N. (2001). Highly efficient gene delivery by mRNA electroporation in human hematopoietic cells: Superiority to lipofection and passive pulsing of mRNA and to electroporation of plasmid cDNA for tumor antigen loading of dendritic cells. Blood *98*, 49–56.

Watanabe, K., Ueno, M., Kamiya, D., Nishiyama, A., Matsumura, M., Wataya, T., Takahashi, J.B., Nishikawa, S., Nishikawa, S.-i., Muguruma, K., and Sasai, Y. (2007). A ROCK inhibitor permits survival of dissociated human embryonic stem cells. Nat. Biotechnol. *25*, 681–686.

Weissman, D., Ni, H., Scales, D., Dude, A., Capodici, J., McGibney, K., Abdool, A., Isaacs, S.N., Cannon, G., and Karikó, K. (2000). HIV gag mRNA transfection of dendritic cells (DC) delivers encoded antigen to MHC class I and II molecules, causes DC maturation, and induces a potent human in vitro primary immune response. J. Immunol. *165*, 4710–4717.

Woltjen, K., Michael, I.P., Mohseni, P., Desai, R., Mileikovsky, M., Hämäläinen, R., Cowling, R., Wang, W., Liu, P., Gertsenstein, M., et al. (2009). piggyBac transposition reprograms fibroblasts to induced pluripotent stem cells. Nature *458*, 766–770.

Yisraeli, J.K., and Melton, D.A. (1989). Synthesis of long, capped transcripts in vitro by SP6 and T7 RNA polymerases. Methods Enzymol. *180*, 42–50.

Yoshida, Y., Takahashi, K., Okita, K., Ichisaka, T., and Yamanaka, S. (2009). Hypoxia enhances the generation of induced pluripotent stem cells. Cell Stem Cell *5*, 237–241.

Yu, J., Vodyanik, M.A., Smuga-Otto, K., Antosiewicz-Bourget, J., Frane, J.L., Tian, S., Nie, J., Jonsdottir, G.A., Ruotti, V., Stewart, R., et al. (2007). Induced pluripotent stem cell lines derived from human somatic cells. Science *318*, 1917–1920.

Yu, J., Hu, K., Smuga-Otto, K., Tian, S., Stewart, R., Slukvin, I.I., and Thomson, J.A. (2009). Human induced pluripotent stem cells free of vector and transgene sequences. Science *324*, 797–801.

Zhou, H., Wu, S., Joo, J.Y., Zhu, S., Han, D.W., Lin, T., Trauger, S., Bien, G., Yao, S., Zhu, Y., et al. (2009). Generation of induced pluripotent stem cells using recombinant proteins. Cell Stem Cell *4*, 381–384.

Cell Stem Cell, Volume *7*

Supplemental Information

Highly Efficient Reprogramming to Pluripotency and Directed Differentiation of Human Cells with Synthetic Modified mRNA

Luigi Warren, Philip D. Manos, Tim Ahfeldt, Yuin-Han Loh, Hu Li, Frank Lau, Wataru Ebina, Pankaj K. Mandal, Zachary D. Smith, Alexander Meissner, George Q. Daley, Andrew S. Brack, James J. Collins, Chad Cowan, Thorsten M. Schlaeger, and Derrick J. Rossi

Supporting Information:

Contains 5 Supplemental Figures and figure legends, 3 Supplemental Tables, and 1 Supplemental movie.

Figure S1 is a schematic of how the modified synthetic mRNA is produced. This figure supports data presented in main Figure 1.

Figure S2 shows that modified RNA can be used to express proteins in multiple human cell types (A), the timecourse expression of high and low stability GFPs (B), apoptosis assays over a time course of repeated transfection (C), heatmaps showing microarray data of stress pathways in cells repeat transfected with modified-RNA (D), and genes upregulated after repeat transfection (E). This figure supports main figure 1.

Figure S3 shows that modified RNA expression is maintained during the time course of reprogramming. Also shows an immuno-stained panel of multiple RiPS cells derived from different human cell types. This figure supports main figures 2

Figure S4 shows results from a RiPS cell derivation in which the cells being reprogrammed were not passaged. This figure support main Figure 5.

Figure S5 shows a panel of histology from multiple teratomas. This figure supports main figure 4.

Table S1: Shows table of pluripotency validation assays performed in this study. This table supports data presented in main Figure 4.

Table S2: Oligonucleotides for IVT template construction. This table supports data in main Figure 2.

Table S3: Primers for qRT-PCR analysis of interferon-regulated genes. This table supports data in main Figure 1.

Supplemental Movie 1. Movie shows multiple embryoid bodies from independent RiPS derivations showing beating cardiomyocytes. This movie supports main Figure 4.

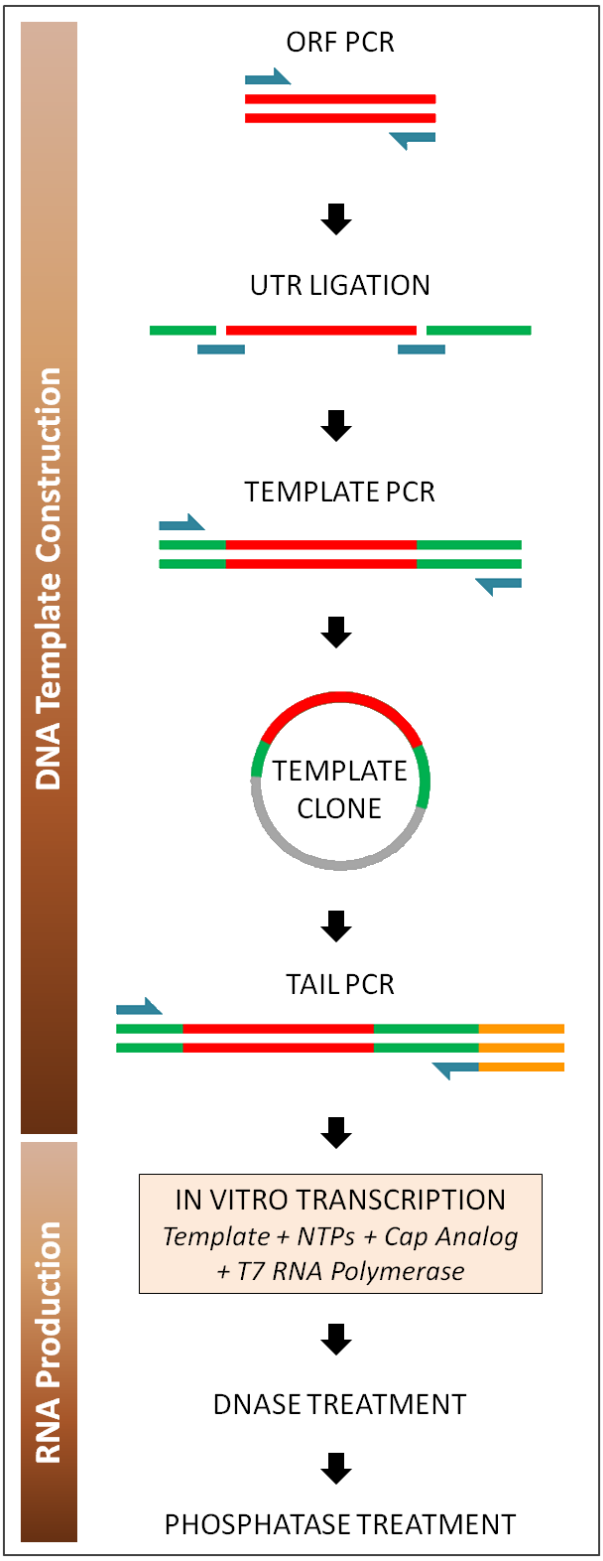

Figure S1 *RNA production flowchart.* To construct a template for RNA transcription reactions, the ORF of a gene of interest is first PCR amplified from a cDNA. Long oligonucleotides containing UTR sequences are then joined to the top strand of ORF amplicons by a thermostable DNA ligase, mediated by annealing to splint oligos which bring the desired single-stranded DNA (ssDNA) ends together. A T7 promoter is incorporated in the 5' UTR fragment. The ssDNA product is amplified using generic primers and TA cloned. A polyA tail is added with a PCR reaction using a T_{120}-heeled reverse primer, and the amplicons are used to template IVT reactions. Modified and unmodified nucleobases are used in the IVT reaction. An anti-reverse di-guanosine cap analog (ARCA) is included in the IVT reaction at four-fold higher concentration than guanosine triphosphate (GTP), as a result of which an estimated 80% of the product is capped. Spin-column purified IVT product is DNase-treated to eliminate the DNA template. Treatment with a phosphatase is used to remove immunonogenic 5' triphosphate moieties from the uncapped RNA fraction. The completed modified-RNA is then re-purified for use in transfections. This figure supports data presented in main Figure 1.

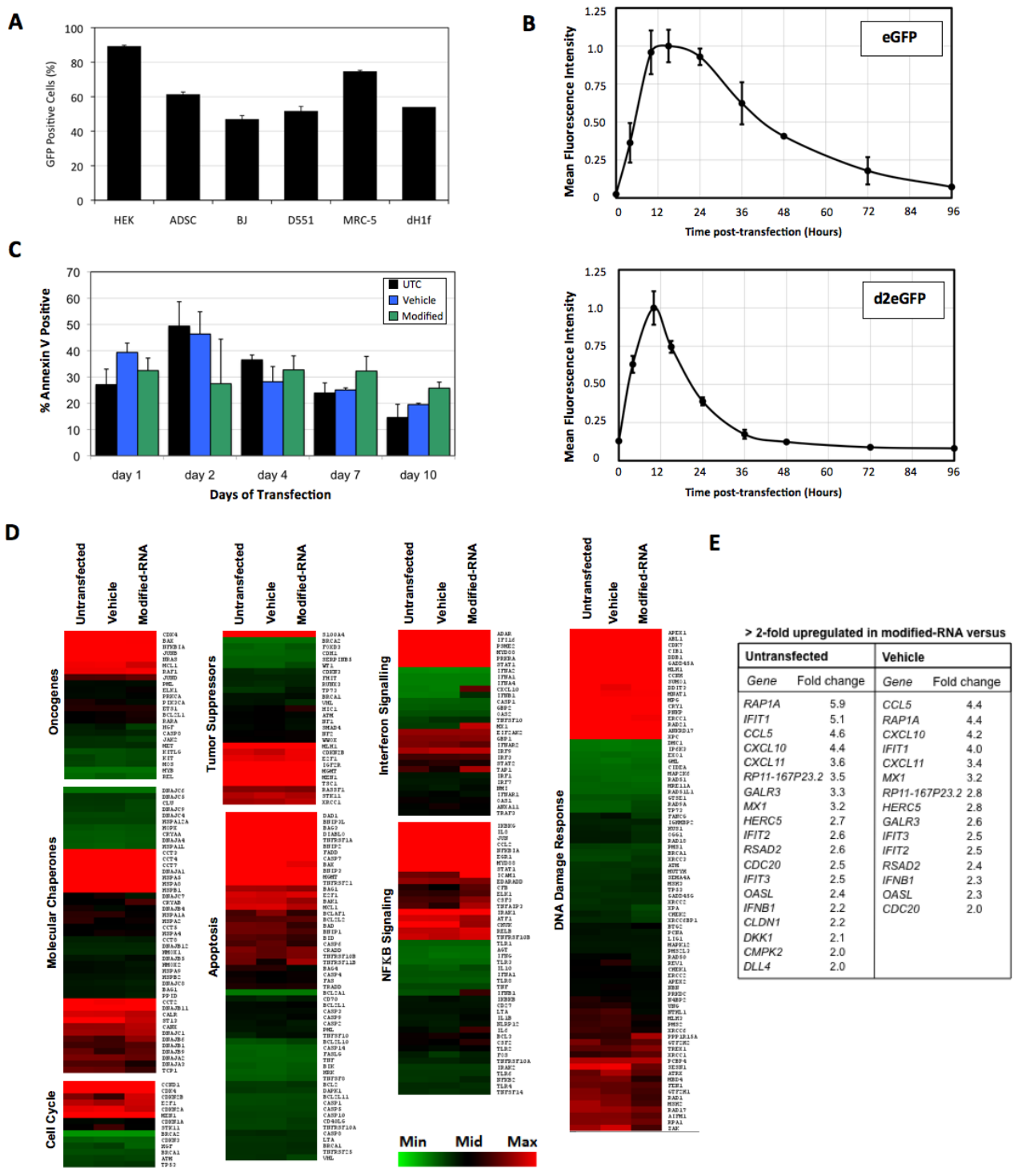

Figure S2 *Penetrant and sustained protein expression mediated by modified-RNA transfection in diverse human cell types, and effects on cell viability and global gene expression.* (A) Flow cytometry analysis showing penetrance of GFP expression 24-hour post-transfection of six human cell types transfected with 1000ng of modified-RNA encoding GFP. Cell types included: human epidermal keratinocytes (HEKs), adipose-derived stem cells (ADSCs), and four different

human fibroblast types (BJ, Detroit 551, MRC-5 and dH1f). Error bars show s.d. for triplicate wells. (B) Expression time courses for cells transfected with modified-RNAs encoding high- and low-stability GFP variants (eGFP and d2eGFP, respectively), assayed by flow cytometry. (C) Annexin V staining at indicated days of BJ fibroblasts transfected daily over the course of 10 days. (D) Heatmap data from microarray analysis of BJ fibroblasts transfected for 10 consecutive days with modified-RNA encoding GFP, vehicle, or untransfected controls. A number of cell stress pathways are shown demonstrating that prolonged transfection with modified RNA does not significantly impact gene the molecular profile of transfected cells beyond upregulation of a number of interferon/NFκB highlighted in (E). (E) All genes upregulated greater than 2-fold in modified-RNA transfected cells versus untransfected cells (right) or vehicle transfected (left) showing induction of number of interferon/NFκB signaling genes consistent with the near but not absolute attenuation of interferon response shown in main Figure 1D. This figure supports data presented in main Figure 1.

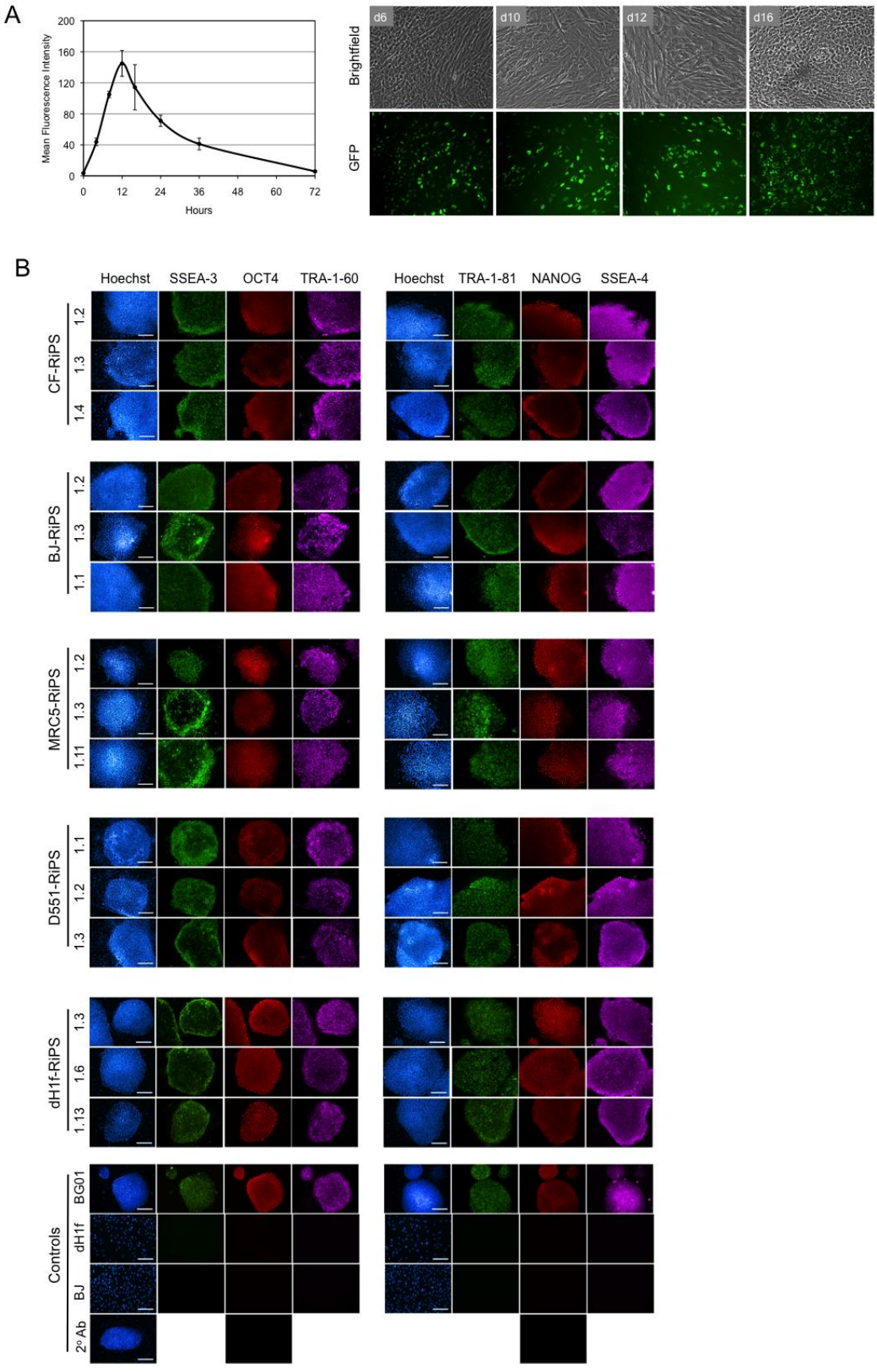
A
Mean Fluorescence Intensity
200
160
120
80
40
0
0
12
24
36
48
60
72
Hours
Brightfield
GFP
d6
d10
d12
d16
B
Hoechst
SSEA-3
OCT4
TRA-1-60
Hoechst
TRA-1-81
NANOG
SSEA-4
CF-RiPS
1.2
1.3
1.4
BJ-RiPS
1.2
1.3
1.1
MRC5-RiPS
1.2
1.3
1.11
D551-RiPS
1.1
1.2
1.3
dH1f-RiPS
1.3
1.6
1.13
Controls
BG01
dH1f
BJ
2° Ab

Figure S3 *iPS-derivation from five human cell types*. (A) Expression time course of low-stability nuclear GFP after a single transfection into keratinocytes, assessed by flow cytometry (right panel). Bright-field and GFP images (right panel) taken at four different time points during a reprogramming experiment. RNA-encoding the low-stability GFP analyzed in the left panel was spiked into the reprogramming cocktail (KMOSL) to visualize sustained protein expression from transfected modified-RNAs during iPS reprogramming (right panel). (B) Antibody stains of independent RiPS clones derived from cells taken from an adult cystic fibrosis patient (CF cells), BJ postnatal fibroblasts, MRC-5 and Detroit 551 fetal fibroblasts, and human ES-derived dH1f fibroblasts. Panels show cell-surface staining for SSEA-3, SSEA-4, TRA-1-60 and TRA-1-81, and intracellular staining for OCT4 and NANOG. Control stains of BG01 hES cells, dH1f and BJ fibroblasts are shown. Additional control stains show the specificity of the secondary antibody used for the OCT4 and NANOG intracellular stains. This figure supports data presented in main Figure 2.

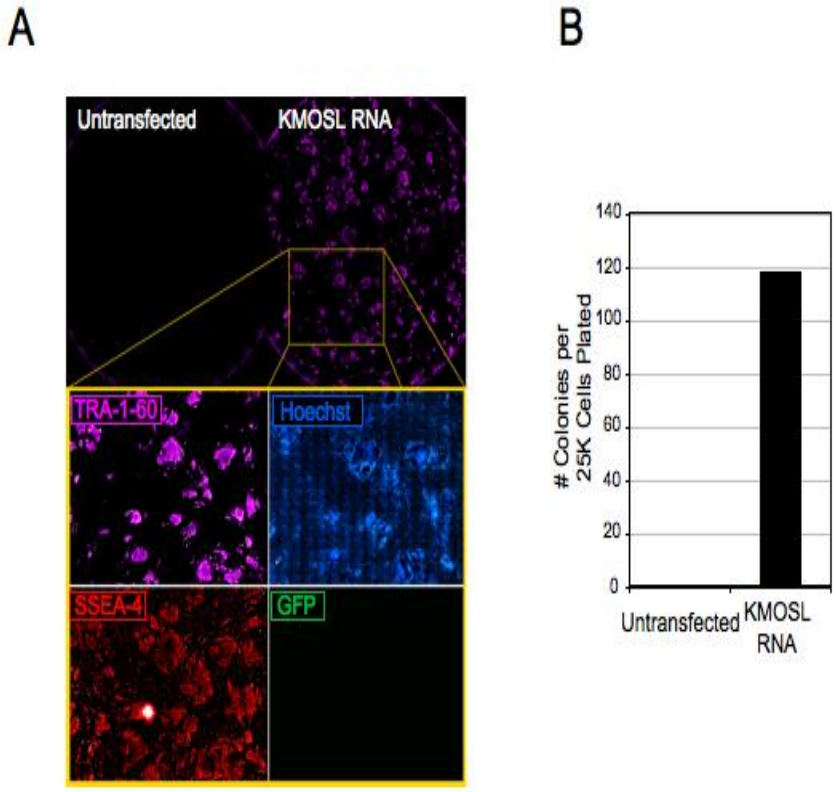

Figure S4 *Efficient RiPS derivation from BJ fibroblasts without passaging*. (A) Immunohistochemistry showing expression of pluripotency markers SSEA-4 and TRA-1-60 in a BJ fibroblast reprogramming experiment transfected for 16 days with 600ng per day of a KMOSL modified RNA cocktail containing a destabilized GFP spike-in. Cultures were fixed for staining at day 18. 50,000 BJ cells were originally seeded onto feeder cells and went unpassaged throughout the course of the experiment. (B) Quantification of TRA-1-60 colony count relative to the number of cells seeded. This figure supports data shown in main Figure 5.

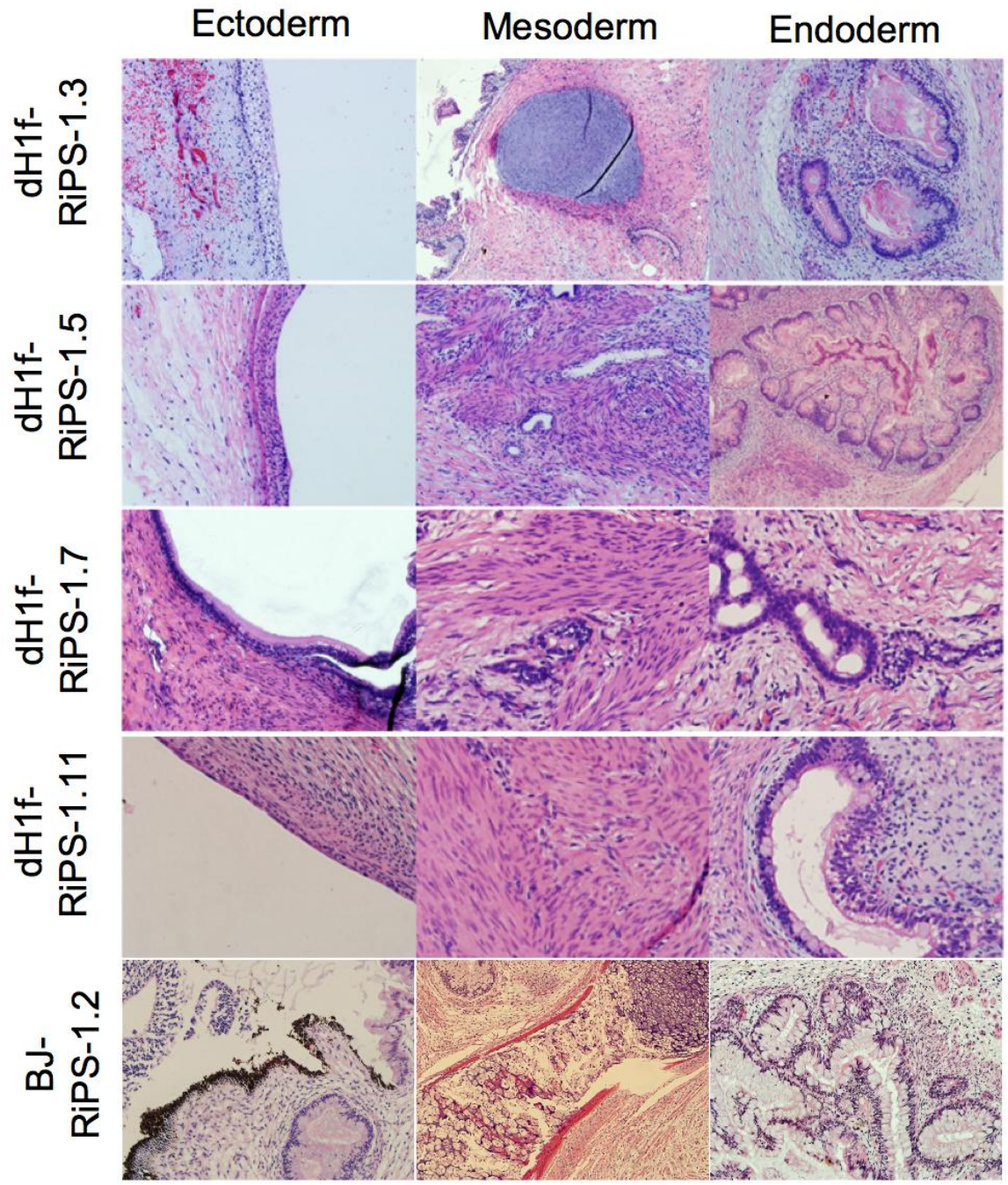

Figure S5 *Teratoma formation and trilineage differentiation of modified-RNA derived iPS clones in vivo.*
(A) Histology of hematoxylin and eosin stained teratomas from the indicated BJ and dH1F RiPS derivations showing structures derived from the three germ layers. This figure supports data shown in main Figure 4.

Immunostaining[#]	qRT-PCR	Bisulfite Sequencing[Ω]	Microarray	Developmental Potential	
				In vitro	Teratoma
dH1F-RiPS-1.3	dH1F-RiPS-1.2	dH1F-RiPS-1.2	dH1F-RiPS-1.2	dH1F-RiPS-1.2^†ø*	dH1F-RiPS-1.3
dH1F-RiPS-1.6	dH1F-RiPS-1.3	dH1F-RiPS-1.3	dH1F-RiPS-1.3	dH1F-RiPS-1.6^ø	dH1F-RiPS-1.5
dH1F-RiPS-1.13	dH1F-RiPS-1.6	dH1F-RiPS-1.6	dH1F-RiPS-1.6	dH1F-RiPS-1.13^ø	dH1F-RiPS-1.6
BJ-RiPS-1.1	dH1F-RiPS-1.7	BJ-RiPS-1.2	dH1F-RiPS-1.7	dH1F-RiPS-1.14^ø	dH1F-RiPS-1.7
BJ-RiPS-1.2	BJ-RiPS-1.1	BJ-RiPS-1.3	BJ-RiPS-1.1	MCR5-RiPS-1.8^†*	dH1F-RiPS-1.11
BJ-RiPS-1.3	BJ-RiPS-1.2	MCR5-RiPS-1.8	BJ-RiPS-1.2	MCR5-RiPS-1.9^†*	BJ-RiPS-1.1
MCR5-RiPS-1.2	BJ-RiPS-1.3	MCR5-RiPS-1.9	BJ-RiPS-1.3	MCR5-RiPS-1.11^*	BJ-RiPS-1.2
MCR5-RiPS-1.3	MCR5-RiPS-1.8	MCR5-RiPS-1.11	MCR5-RiPS-1.8	BJ-RiPS-1.1^†ø*	CF-RiPS-1.4
MCR5-RiPS-1.11	MCR5-RiPS-1.9	CF-RiPS-1.2	MCR5-RiPS-1.9	BJ-RiPS-1.2^†ø*	
CF-RiPS-1.2	MCR5-RiPS-1.11	CF-RiPS-1.3	MCR5-RiPS-1.11	BJ-RiPS-1.3^†*	
CF-RiPS-1.3	CF-RiPS-1.2	CF-RiPS-1.4	CF-RiPS-1.2	CF-RiPS-1.2^†*	
CF-RiPS-1.4	CF-RiPS-1.3		CF-RiPS-1.3	CF-RiPS-1.3^†*	
D551-RiPS-1.1	CF-RiPS-1.4		CF-RiPS-1.4	CF-RiPS-1.4^ø*	
D551-RiPS-1.2	D551-RiPS-1.1			D551-RiPS-1.1^†*	
D551-RiPS-1.3	D551-RiPS-1.2			D551-RiPS-1.2^*	
	D551-RiPS-1.3			D551-RiPS-1.3^*	

Table S1: *Pluripotency validation assays performed in this study.* The table shows the RiPS clones that were validate in each assay. # Validated for immuno-staining for all of TRA-1-60, TRA-1-80, SSEA3, SSEA4, OCT4, NANOG. [Ω] Demethylation of the *OCT4* promoter. *In vitro* differentiation including ^embryoid body formation, [ø]trilineage by directed differentiation, [†] beating cardiomyocytes, and * blood formation by CFC assays in methylcellulose. This table supports data presented in main Figure 4.

	ORF Forward Primer	ORF Reverse Primer
eGFP	GTGAGCAAGGGCGAGGAGCTGTT	TTACTTGTACAGCTCGTCCATGCCGAGA
d2eGFP	GTGAGCAAGGGCGAGGAGCTGTT	CTACACATTGATCCTAGCAGAAGCACAGGCT
KLF4	GCTGTCAGCGACGCGCTGCTC	TTAAAAATGCCTCTTCATGTGTAAGGCGAGGT
c-MYC	CCCCTCAACGTTAGCTTCACCAACAGG	TTACGCACAAGAGTTCCGTAGCTGTTCA
OCT4	GCGGGACACCTGGCTTCGGATTTC	TCAGTTTGAATGCATGGGAGAGCCCAGA
SOX2	TACAACATGATGGAGACGGAGCTGAAGC	TCACATGTGTGAGAGGGGCAGTGTG
LIN28	GGCTCCGTGTCCAACCAG	TCAATTCTGTGCCTCCGG
MYOD	GAGCTTCTATCGCCGCCACTCC	TCAAAGCACCTGATAAATCGCATTGG
	5' Splint Oligo	**3' Splint Oligo**
eGFP	TCCTCGCCCTTGCTCACCATGGTGGCTCTTATATTTCTTCTT	CCCGCAGAAGGCAGCTTACTTGTACAGCTCGTCCATGC
d2eGFP	TCCTCGCCCTTGCTCACCATGGTGGCTCTTATATTTCTTCTT	CCCGCAGAAGGCAGCCTACACATTGATCCTAGCAGA
KLF4	GCGCGTCGCTGACAGCCATGGTGGCTCTTATATTTCTTCTT	CCCGCAGAAGGCAGCTTAAAAATGCCTCTTCATGTGTAA
c-MYC	GTGAAGCTAACGTTGAGGGGCATGGTGGCTCTTATATTTCTTCTT	CCCGCAGAAGGCAGCTTACGCACAAGAGTTCCGTAG
OCT4	AAGCCAGGTGTCCCGCCATGGTGGCTCTTATATTTCTTCTT	CCCGCAGAAGGCAGCTCAGTTTGAATGCATGGGAG
SOX2	CTCCGTCTCCATCATGTTGTACATGGTGGCTCTTATATTTCTTCTT	CCCGCAGAAGGCAGCTCACATGTGTGAGAGGGGC
LIN28	CTGGTTGGACACGGAGCCCATGGTGGCTCTTATATTTCTTCTT	CCCGCAGAAGGCAGCTCAATTCTGTGCCTCCGG
MYOD	TGGCGGCGATAGAAGCTCCATGGTGGCTCTTATATTTCTTCTT	CCCGCAGAAGGCAGCTCAAAGCACCTGATAAATCGCATTGG
	UTR Oligos	
5' UTR	TTGGACCCTCGTACAGAAGCTAATACGACTCACTATAGGGAAATAAGAGAGAAAAGAAGAGTAAGAAGAAATATAAGAGCCACCATG	
3' UTR	GCTGCCTTCTGCGGGGCTTGCCTTCTGGCCATGCCCTTCTTCTCTCCCTTGCACCTGTACCTCTTGGTCTTTGAATAAAGCCTGAGTAGGAAGTGAGGGTCTAGAACTAGTGTCGACGC	
	Forward Primer	**Reverse Primer**
Template PCR	TTGGACCCTCGTACAGAAGCTAATACG	GCGTCGACACTAGTTCTAGACCCTCA
Tail PCR	TTGGACCCTCGTACAGAAGCTAATACG	T_{120}CTTCCTACTCAGGCTTTATTCAAAGACCA

Table S2 *Oligonucleotides for IVT template construction.* 5’ and 3’ UTR oligos are ligated to the top strand of gene-specific ORF amplicons to produce a basic template construct for cloning (Supplemental Figure S1). Underlined bases in the 5’ UTR oligo sequence indicate the upstream T7 promoter, and in the 3’ UTR oligo sequence show downstream restriction sites, introduced to facilitate linearization of template plasmids. Template PCR primers are used to amplify ligation products for sub-cloning. Tail PCR primers are used to append an oligo(dT) sequence immediately after the 3’ UTR to drive templated addition of a poly(A) tail during IVT reactions. Gene-specific ORF primers are used to capture the coding region (minus the start codon) from cDNA templates. Splint oligos mediate ligation of UTR oligos to the top strand of ORF amplicons. This table supports data in main Figure 2.

Transcript	Forward Primer	Reverse Primer
GAPDH	GAAGGCTGGGGCTCATTT	CAGGAGGCATTGCTGATGAT
IFNA	ACCCACAGCCTGGATAACAG	ACTGGTTGCCATCAAACTCC
IFNB	CATTACCTGAAGGCCAAGGA	CAGCATCTGCTGGTTGAAGA
IFIT1	AAAAGCCCACATTTGAGGTG	GAAATTCCTGAAACCGACCA
OAS1	CGATCCCAGGAGGTATCAGA	TCCAGTCCTCTTCTGCCTGT
PKR	TCGCTGGTATCACTCGTCTG	GATTCTGAAGACCGCCAGAG
RIG-I	GTTGTCCCCATGCTGTTCTT	GCAAGTCTTACATGGCAGCA

Table S3 *Primers for qRT-PCR analysis of interferon-regulated genes*. This table supports data in main Figure 1.

Movie S1 *Embryoid bodies from independent RiPS derivations showing beating cardiomyocytes*. Top row (left to right) BJ-RiPS1.1, BJ-RiPS1.2 and BJ-RiPS1.3 Middle row (left to right) CF-RiPS1.3, D551-RiPS1.2, MRC5-RiPS1.8, Bottom row (left to right) CF-RiPS1.4, D551-RiPS1.3, MRC5-RiPS1.9. This movie supports main figure 4. Movie available online.